[Short title + Author Name - P&H title] 17 (2024) 105872

Contents lists available at ScienceDirect

Arabian Journal of Chemistry

journal homepage: www.ksu.edu.sa

Preparation and biological evaluation of coumarin amide derivatives bearing fluorine as potential fungicides and anticancer agents

Xin Xiang [1], Yafang Chen [1], Lang Wu, Long Zhang, Yan Zhang, Wude Yang [*], Xiang Yu [*]

College of Pharmacy, Guizhou University of Traditional Chinese Medicine, Guiyang 550025, China

ARTICLE INFO

Keywords:
Coumarin
Fluorine
Synthesis
Antifungal activities
Anticancer activity

ABSTRACT

In order to find new potential fungicides and anticancer agents, a series of new coumarin amide derivatives bearing fluorine were synthesized and characterized spectroscopically. Compounds **A6**, **B11**, **C2** and **C7** were confirmed by X-ray diffraction further. The antifungal bioassays against five typical pathogenic fungi showed that compound **C5** exhibited more remarkable fungicidal activities against *Alternaria alternata* (EC_{50} = 11.5 μg/mL), *Colletotrichum gloeosporioides* (EC_{50} = 18.0 μg/mL), *Pyricularia grisea* (EC_{50} = 33.8 μg/mL), surpassing kresoxim-methyl. Molecular docking result indicated that **C5** displayed high binding affinity to chitinase, which plays crucial role in degradation and remodeling of fungal cell walls. In addition, the anticancer bioassays against three cancer cells demonstrated that compound **A4** displayed excellent growth inhibitory effect against Hela cells with IC_{50} value of 8.13 μM, and low cytotoxicity against human normal cells BEAS-2B. Flow cytometric analysis further demonstrated that **A4** significantly arrested cell cycle at the S phase and trigger apoptosis. With the above interesting biological profile, these coumarin derivatives could be used as anfungicides and anticancer candidates.

1. Introduction

The natural compound coumarin, and its derivatives, can be found in many species of plants, particularly Rutaceae and Apiaceae (Santos Junior et al., 2023). They are classified into four groups: simple coumarins, furanocoumarins, pyranocoumarins, and pyrone-substituted coumarins (Fig. 1, **I** ~ **IV**) (Küpeli Akkol et al., 2020). These compounds have been used for the benefit of humankind, including in medical and agrochemical applications (Akwu et al., 2023; Prusty and Kumar, 2020). In the field of medicinal chemistry, coumarin and its derivatives represent one of the most important skeletons of pharmaceutically active compounds, exhibiting a broad spectrum of medicinal activities. These activities include antitumor (Sakunpak et al., 2013; Maleki et al., 2020; Phutdhawong et al., 2021), antiviral activity (Tang et al., 2016; Liu et al., 2020), antibacterial (Zuo et al., 2016; Tan et al., 2017), antioxidant (Bizzarri et al., 2017; Kassim et al., 2013), neuroprotective (Huang et al., 2021; Yu et al., 2021), anti-inflammatory (Lv et al., 2015; Tuan Anh et al., 2017), Anticoagulant (Awaad et al., 2012; Gao et al., 2021), and more. In the agrochemical field, they also demonstrate a wide range of agro-activities, such as insecticidal (Siskos et al., 2008; Yang et al., 2022; Ma et al., 2024) and antifungal properties (Li et al., 2023; Song et al., 2017).

Moreover, fluorine is a small atom with a van der Waals radius, positioned between hydrogen and oxygen, making it suitable to imitate a hydroxyl group and participate in hydrogen bonding interactions (Hunter, 2010; Ismail, 2002). Introducing fluorine into compounds can modulate physicochemical properties such as pharmacological properties, lipophilicity, metabolic stability, membrane permeability, and binding affinity (Purser et al., 2008). Previous studies have shown that organo-fluorine can be used not only in anticancer (Longley et al., 2003; Duan et al., 2013), anti-inflammatory (Luan et al., 2023; Deshpande and Pai, 2012) and antiviral agents (Han and Lu, 2023; Cavaliere et al., 2017), but also in the development of pesticides (Jeschke, 2017; Jeschke, 2004). Furthermore, many active drugs on the market contain fluorine, such as fluorouracil (Alzahrani et al., 2023), emtricitabine (Deeks, 2018), teriflunomide (Paik, 2021) and tavaborale (Poulakos et al., 2017) (Fig. 1, **V** ~ **VIII**).

Molecular hybridization involves the fusion of the chemical structures of two drugs to create a single molecule, or the integration of the pharmacological components of both drugs into a hybrid molecule.

* Corresponding authors.
E-mail addresses: yangwude476@gzy.edu.cn (W. Yang), yuxiang@gzy.edu.cn (X. Yu).
[1] These authors contribute equally to this work.

https://doi.org/10.1016/j.arabjc.2024.105872
Received 25 April 2024; Accepted 10 June 2024
Available online 11 June 2024

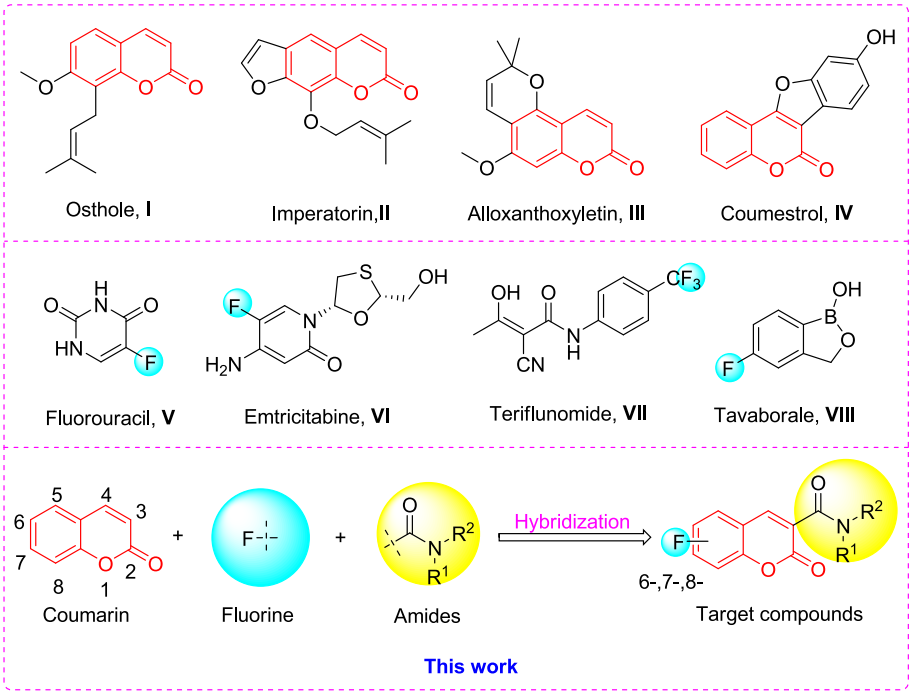

Fig. 1. Design of the coumarin amide derivatives bearing fluorine.

These newly formed hybrid molecules, which combine the therapeutic properties of both drugs, enhance their pharmacological efficacy and mitigate their potential adverse effects. Alternatively, hybrid molecules can leverage the strengths and weaknesses of each drug to synergistically enhance their respective pharmacological activities and optimize the treatment outcome. It has become one of the current trends in the development of biologically active compounds (Zhao et al., 2023; Yang et al., 2024). Given the aforementioned facts, as shown in Fig. 1, in this study, we designed new fungicides and anticancer compounds by combining coumarin with fluorine and an amide moiety, and tested their in vitro antifungal activities against five phytopathogenic fungi, including *Alternaria brassicae* (AB), *Alternaria alternata* (AA), *Colletotrichum gloeosporioides* (CG), *Pyricularia grisea* (PG), *Fusarium oxysporium f. sp.vasinfectum* (FV) and antiproliferative effect against human cervical cancer cell line (HeLa), human hepatoma cancer cell line (HepG2), and human colorectal cancer cell line (HCT116). The preliminary anticancer mechanism of the powerful compounds was also examined using tests that evaluate the distribution of the cells in the phases of the cell cycle and the induction of apoptosis.

2. Materials and methods

2.1. General experimental

Thin-layer chromatography (TLC) was performed on silica gel plates using silica gel 60 GF254 (Qingdao Haiyang Chemical Co., Ltd., Qingdao, China). Melting points were determined on The X-5A micro melting point tester (Gongyi Kerui instrument Co., Ltd). NMR spectra were performed on a Bruker Avance neo 400 MHz instrument (Bruker, Bremerhaven, Germany). HRMS was performed on Xevo G2-SQTOF instrument (Waters, Milford, MA, USA).

2.1.1. Synthesis of the intermediates **5a ~ c**

The different coumarin-3-formyl chlorides **5a ~ c** were prepared as previous literature (Zhang et al., 2018). Firstly, fluorosalicylaldehydes compounds (**1a ~ c**) (80 mmol), diethyl malonate (96 mmol) and catalytic amounts of piperidine (1 mL) were refluxed in ethanol for 2 h. After cooling to room temperature, the suspension was filtered off and **3a ~ c** was attained. Afterwards, compound **3a ~ c** was hydrolyzed in ethanolic solution with 2 N NaOH (aq.) at reflux for 30 min. After reaction, 2 N HCl (aq.) was added and acids **4a ~ c** were obtained by filtering the white precipitate, washing it with water, and then drying it. Finally, the solution of compounds **4a ~ c** (10 mmol) in dichloromethane (DCM, 100 mL) was added two drops dimethylformamide (DMF), and oxalyl chloride (13 mmol) slowly. The blend was agitated at ambient temperature for 8 h, then concentrated after completion of the reaction to yield compounds **5a ~ c**.

2.1.2. Synthesis of compounds **A1 ~ 9, B1 ~ 14, C1 ~ 11**

A mixture of compounds **5a ~ c** (0.5 mmol), amines (0.5 mmol), triethylamine (6 mmol) in tetrahydrofuran (THF, 20 mL) was stirred at 50 °C overnight. The reaction mixture was diluted with 30 mL of ethyl acetate, followed by washing with saturated $NaHCO_3$ solution (3 × 30 mL), saturated saline solution (50 mL), and drying with anhydrous Na_2SO_4. After evaporating the organic phase, the residues were purified using silica gel column chromatography (petroleum ether: ethyl acetate = 1: 1) to isolate the desired compounds **A1 ~ 9**, **B1 ~ 14**, **C1 ~ 11**.

2.1.2.1. N-ethyl-6-fluoro-2-oxo-2H-chromene-3-carboxamide ***(A1).*** Yield: 66 %, white solid, mp 183–184 °C; ^{1}H NMR (400 MHz, $CDCl_3$) δ 8.87 (s, 1H), 8.75 (s, 1H), 7.47 – 7.30 (m, 3H), 3.51 (p, J = 6.9 Hz, 2H), 1.27 (t, J = 7.2 Hz, 3H); ^{13}C NMR (101 MHz, $CDCl_3$) δ 161.0, 160.8, 160.2 (d, J = 246.7 Hz), 150.5, 147.1, 121.6 (d, J = 24.7 Hz), 119.6, 119.4 (d, J = 9.6 Hz), 118.3 (d, J = 8.9 Hz), 114.7 (d, J = 23.6 Hz), 34.8, 14.6; HRMS (ESI) calcd for $C_{12}H_{11}O_3NF$ ([M + H]$^+$) 236.0717, found 236.0713.

2.1.2.2. N-butyl-6-fluoro-2-oxo-2H-chromene-3-carboxamide ***(A2).*** Yield: 77 %, yellow solid, mp 162–163 °C; ^{1}H NMR (400 MHz, $CDCl_3$) δ 8.86 (s, 1H), 8.78 (s, 1H), 7.47 – 7.31 (m, 3H), 3.47 (q, J = 6.8 Hz, 2H), 1.67 – 1.59 (m, 2H), 1.43 (h, J = 7.3 Hz, 2H), 0.96 (t, J = 7.3 Hz, 3H); ^{13}C NMR (101 MHz, $CDCl_3$) δ 161.0, 160.9, 160.2 (d, J = 247.3 Hz), 150.5 (d, J = 1.5 Hz), 147.1 (d, J = 2.9 Hz), 121.6 (d, J = 24.7 Hz), 119.6, 119.4 (d, J = 9.2 Hz), 118.3 (d, J = 8.2 Hz), 114.7 (d, J = 23.6 Hz), 39.7, 31.4, 20.1, 13.7; HRMS (ESI) calcd for $C_{14}H_{15}O_3NF$ ([M + H]$^+$) 264.1030, found 264.1026.

*2.1.2.3. 6-fluoro-N-isopropyl-2-oxo-2H-chromene-3-carboxamide **(A3)***. Yield: 80 %, white solid, mp 169–170 °C; ^{1}H NMR (400 MHz, $CDCl_3$) δ 8.86 (s, 1H), 8.64 (s, 1H), 7.43 – 7.33 (m, 3H), 4.30 – 4.21 (m, 1H), 1.28 (d, J = 6.6 Hz, 6H); ^{13}C NMR (101 MHz, $CDCl_3$) δ 161.0, 160.2 (d, J = 247.2 Hz), 160.0, 150.5 (d, J = 2.1 Hz), 147.1 (d, J = 2.9 Hz), 121.6 (d, J = 24.8 Hz), 119.7, 119.4 (d, J = 9.4 Hz), 118.3 (d, J = 8.6 Hz), 114.7 (d, J = 23.9 Hz), 42.0, 22.5 × 2; HRMS (ESI) calcd for $C_{13}H_{13}O_3NF$ ([M + H]$^+$) 250.0874, found 250.0869.

*2.1.2.4. 6-fluoro-2-oxo-N-(pentan-3-yl)–2H-chromene-3-carboxamide **(A4)***. Yield: 59 %, white solid, mp 141–142 °C; ^{1}H NMR (400 MHz, $CDCl_3$) δ 8.87 (s, 1H), 8.59 (s, 1H), 7.51 – 7.33 (m, 3H), 4.04 – 3.95 (m, 1H), 1.73 – 1.52 (m, 4H), 0.96 (t, J = 7.4 Hz, 6H); ^{13}C NMR (101 MHz, $CDCl_3$) δ 161.1, 160.7, 160.2 (d, J = 246.9 Hz), 150.5 (d, J = 1.6 Hz), 147.2 (d, J = 2.9 Hz), 121.5 (d, J = 24.7 Hz), 119.7, 119.4 (d, J = 9.4 Hz), 118.2 (d, J = 8.9 Hz), 114.7 (d, J = 23.9 Hz), 52.7, 27.2 × 2, 10.2 × 2; HRMS (ESI) calcd for $C_{15}H_{17}O_3NF$ ([M + H]$^+$) 278.1187, found 278.1179.

*2.1.2.5. N-cyclopropyl-6-fluoro-2-oxo-2H-chromene-3-carboxamide **(A5)***. Yield: 65 %, white solid, mp 193–195 °C; ^{1}H NMR (400 MHz, $CDCl_3$) δ 8.88 (s, 1H), 8.78 (s, 1H), 7.45 – 7.33 (m, 3H), 2.99 – 2.93 (m, 1H), 0.91 – 0.86 (m, 2H), 0.72 – 0.60 (m, 2H); ^{13}C NMR (101 MHz, $CDCl_3$) δ 162.3, 160.9, 160.2 (d, J = 247.2 Hz), 150.5 (d, J = 1.6 Hz), 147.1 (d, J = 2.9 Hz), 121.7 (d, J = 24.8 Hz), 119.4, 119.3 (d, J = 9.2 Hz), 118.3 (d, J = 8.2 Hz), 114.7 (d, J = 23.8 Hz), 23.0, 6.6 × 2; HRMS (ESI) calcd for $C_{13}H_{11}O_3NF$ ([M + H]$^+$) 248.0717, found 248.0713.

*2.1.2.6. N-cyclohexyl-6-fluoro-2-oxo-2H-chromene-3-carboxamide **(A6)***. Yield: 86 %, yellow solid, mp 217–218 °C; ^{1}H NMR (400 MHz, $CDCl_3$) δ 8.86 (s, 1H), 8.74 (s, 1H), 7.46 – 7.31 (m, 3H), 4.02 – 3.94 (m, 1H), 2.05 – 1.94 (m, 2H), 1.80 – 1.63 (m, 3H), 1.48 – 1.25 (m, 5H); ^{13}C NMR (101 MHz, $CDCl_3$) δ 161.0, 160.2 (d, J = 247.2 Hz), 159.9,150.5, 147.2 (d, J = 3.1 Hz), 121.5 (d, J = 24.8 Hz), 119.8, 119.4 (d, J = 9.5 Hz), 118.2 (d, J = 8.2 Hz), 114.7 (d, J = 23.7 Hz), 48.6, 32.7 × 2, 25.5, 24.6 × 2; HRMS (ESI) calcd for $C_{16}H_{17}O_3NF$ ([M + H]$^+$) 290.1187, found 290.1181.

*2.1.2.7. N-cycloheptyl-6-fluoro-2-oxo-2H-chromene-3-carboxamide **(A7)***. Yield: 69 %, yellow solid, mp 183–184 °C; ^{1}H NMR (400 MHz, $CDCl_3$) δ 8.85 (s, 1H), 8.78 (s, 1H), 7.50 – 7.32 (m, 3H), 4.20 – 4.12 (m, 1H), 2.07 – 1.94 (m, 2H), 1.71 – 1.56 (m, 10*H*); ^{13}C NMR (101 MHz, $CDCl_3$) δ 161.0, 160.2 (d, J = 246.9 Hz), 159.6, 150.5, 147.2 (d, J = 2.9 Hz), 121.5 (d, J = 24.7 Hz), 119.9, 119.4 (d, J = 9.3 Hz), 118.2 (d, J = 8.4 Hz), 114.7 (d, J = 23.5 Hz), 50.9, 34.7 × 2, 27.9 × 2, 24.1 × 2; HRMS (ESI) calcd for $C_{17}H_{19}O_3NF$ ([M + H]$^+$) 304.1343, found 304.1337.

*2.1.2.8. 6-fluoro-N-methyl-2-oxo-N-phenyl-2H-chromene-3-carboxamide **(A8)***. Yield: 68 %, yellow solid, mp 219–220 °C; ^{1}H NMR (400 MHz, $CDCl_3$) δ 7.64 (s, 1H), 7.30 – 7.19 (m, 7H), 7.10 (d, J = 7.9 Hz, 1H), 3.48 (s, 3H); ^{13}C NMR (101 MHz, $CDCl_3$) δ 164.4, 159.9 (d, J = 246.0 Hz), 157.1, 149.9, 142.8, 141.0, 129.4 × 2, 127.8, 127.2, 126.9 × 2, 120.0 (d, J = 24.7 Hz), 118.7 (d, J = 9.1 Hz), 118.3 (d, J = 8.3 Hz), 113.6 (d, J = 23.9 Hz), 37.5; HRMS (ESI) calcd for $C_{17}H_{13}O_3NF$ ([M + H]$^+$) 298.0874, found 298.0873.

*2.1.2.9. 6-fluoro-N-(2-methoxyphenyl)-2-oxo-2H-chromene-3-carboxamide **(A9)***. Yield: 73 %, white solid, mp 234–235 °C; ^{1}H NMR (400 MHz, $CDCl_3$) δ 11.26 (s, 1H), 8.94 (s, 1H), 8.53 (d, J = 9.2 Hz, 1H), 7.46 – 7.36 (m, 3H), 7.12 (t, J = 7.1 Hz, 1H), 7.01 (t, J = 7.3 Hz, 1H), 6.95 (d, J = 8.1 Hz, 1H), 3.98 (s, 3H); ^{13}C NMR (101 MHz, $CDCl_3$) δ 161.0, 160.3 (d, J = 247.5 Hz), 158.6, 150.6, 149.1, 147.5 (d, J = 2.9 Hz), 127.5, 124.7, 121.8 (d, J = 24.7 Hz), 121.0, 120.7, 120.2, 119.4 (d, J = 9.3 Hz), 118.4 (d, J = 8.4 Hz), 114.8 (d, J = 23.8 Hz), 110.2, 56.0; HRMS (ESI) calcd for $C_{17}H_{13}O_4NF$ ([M + H]$^+$) 314.0823, found 314.0816.

*2.1.2.10. N-ethyl-7-fluoro-2-oxo-2H-chromene-3-carboxamide **(B1)***. Yield: 60 %, white solid, mp 171–173 °C; ^{1}H NMR (400 MHz, $CDCl_3$) δ 8.89 (s, 1H), 8.68 (s, 1H), 7.72 – 7.68 (m, 1H), 7.15 – 7.10 (m, 2H), 3.53 (p, J = 7.1 Hz, 2H), 1.27 (t, J = 7.1 Hz, 3H); ^{13}C NMR (101 MHz, $CDCl_3$) δ 166.2 (d, J = 258.8 Hz), 160.2 × 2, 154.8 (d, J = 13.7 Hz), 146.7, 130.8 (d, J = 10.7 Hz), 116.7 (d, J = 3.9 Hz), 114.6 (d, J = 2.7 Hz), 113.6 (d, J = 23.5 Hz), 103.6 (d, J = 25.8 Hz), 33.9, 13.8; HRMS (ESI) calcd for $C_{12}H_{11}O_3NF$ ([M + H]$^+$) 236.0717, found 236.0713.

*2.1.2.11. 7-fluoro-2-oxo-N-propyl-2H-chromene-3-carboxamide **(B2)***. Yield: 59 %, white solid, mp 164–166 °C; ^{1}H NMR (400 MHz, $CDCl_3$) δ 8.89 (s, 1H), 8.72 (s, 1H), 7.72 – 7.68 (m, 1H), 7.22 – 7.01 (m, 2H), 3.51 – 3.38 (m, 2H), 1.66 (h, J = 7.3 Hz, 2H), 1.00 (t, J = 7.4 Hz, 3H); ^{13}C NMR (101 MHz, $CDCl_3$) δ 167.1 (d, J = 258.7 Hz), 161.2, 161.0, 155.7 (d, J = 13.7 Hz), 147.5, 131.6 (d, J = 10.4 Hz), 117.4 (d, J = 3.3 Hz), 115.4 (d, J = 2.7 Hz), 113.8 (d, J = 23.2 Hz), 104.4 (d, J = 25.9 Hz), 41.6, 22.6, 11.4; HRMS (ESI) calcd for $C_{13}H_{13}O_3NF$ ([M + H]$^+$) 250.0874, found 250.0868.

*2.1.2.12. N-butyl-7-fluoro-2-oxo-2H-chromene-3-carboxamide **(B3)***. Yield: 71 %, white solid, mp 146–148 °C; ^{1}H NMR (400 MHz, $CDCl_3$) δ 8.89 (s, 1H), 8.73 (s, 1H), 7.77 – 7.68 (m, 1H), 7.17 – 7.09 (m, 2H), 3.52 – 3.43 (m, 2H), 1.62 (p, J = 7.4 Hz, 2H), 1.47 – 1.38 (m, 2H), 0.96 (t, J = 7.4 Hz, 3H); ^{13}C NMR (101 MHz, $CDCl_3$) δ 167.1 (d, J = 259.1 Hz), 161.2, 161.0, 155.7 (d, J = 13.3 Hz), 147.5, 131.6 (d, J = 10.8 Hz), 117.4 (d, J = 3.4 Hz), 115.4 (d, J = 1.8 Hz), 113.9 (d, J = 23.0 Hz), 104.4 (d, J = 25.7 Hz), 39.6, 31.4, 20.1, 13.7; HRMS (ESI) calcd for $C_{14}H_{15}O_3NF$ ([M + H]$^+$) 264.1030, found 264.1025.

*2.1.2.13. 7-fluoro-N-hexyl-2-oxo-2H-chromene-3-carboxamide **(B4)***. Yield: 59 %, yellow solid, mp 132–134 °C; ^{1}H NMR (400 MHz, $CDCl_3$) δ 8.82 (s, 1H), 8.64 (s, 1H), 7.65 – 7.61 (m, 1H), 7.11 – 6.96 (m, 2H), 3.38 (q, J = 7.0 Hz, 2H), 1.55 (p, J = 7.2 Hz, 2H), 1.35 – 1.22 (m, 6H), 0.82 (t, J = 6.8 Hz, 3H); ^{13}C NMR (101 MHz, $CDCl_3$) δ 167.1 (d, J = 256.3 Hz), 161.1, 161.0, 155.7 (d, J = 12.9 Hz), 147.5, 131.6 (d, J = 11.2 Hz), 117.4 (d, J = 2.5 Hz), 115.4 (d, J = 2.5 Hz), 113.8 (d, J = 23.3 Hz), 104.4 (d, J = 26.5 Hz), 39.9, 31.4, 29.3, 26.6, 22.5, 13.9; HRMS (ESI) calcd for $C_{16}H_{19}O_3NF$ ([M + H]$^+$) 292.1343, found 292.1339.

*2.1.2.14. 7-fluoro-N-isopropyl-2-oxo-2H-chromene-3-carboxamide **(B5)***. Yield: 76 %, yellow solid, mp 176–178 °C; ^{1}H NMR (400 MHz, $CDCl_3$) δ 8.88 (s, 1H), 8.56 (s, 1H), 7.72 – 7.68 (m, 1H), 7.17 – 7.05 (m, 2H), 4.31 – 4.20 (m, 1H), 1.28 (d, J = 6.6 Hz, 6H); ^{13}C NMR (101 MHz, $CDCl_3$) δ 167.0 (d, J = 258.3 Hz), 161.0, 160.2, 155.7 (d, J = 13.2 Hz), 147.5, 131.6 (d, J = 10.8 Hz), 117.6 (d, J = 3.0 Hz), 115.5 (d, J = 2.8 Hz), 113.8 (d, J = 23.2 Hz), 104.4 (d, J = 26.2 Hz), 41.9, 22.5 × 2; HRMS (ESI) calcd for $C_{13}H_{13}O_3NF$ ([M + H]$^+$) 250.0874, found 250.0868.

*2.1.2.15. N-cyclopropyl-7-fluoro-2-oxo-2H-chromene-3-carboxamide **(B6)***. Yield: 82 %, white solid, mp 190–192 °C; ^{1}H NMR (400 MHz, $CDCl_3$) δ 8.90 (s, 1H), 8.71 (s, 1H), 7.72 – 7.68 (m, 1H), 7.21 – 7.07 (m, 2H), 2.99 – 2.92 (m, 1H), 0.90 – 0.85 (m, 2H), 0.69 – 0.63 (m, 2H); ^{13}C NMR (101 MHz, $CDCl_3$) δ 167.1 (d, J = 259.5 Hz), 162.5, 161.0, 155.7 (d, J = 13.8 Hz), 147.5, 131.7 (d, J = 10.5 Hz), 117.2 (d, J = 3.4 Hz), 115.4 (d, J = 2.1 Hz), 113.8 (d, J = 22.8 Hz), 104.4 (d, J = 25.6 Hz), 22.9, 6.6 × 2; HRMS (ESI) calcd for $C_{13}H_{11}O_3NF$ ([M + H]$^+$) 248.0717, found 248.0712.

*2.1.2.16. N-cyclohexyl-7-fluoro-2-oxo-2H-chromene-3-carboxamide **(B7)***. Yield: 64 %, yellow solid, mp 202–204 °C; ^{1}H NMR (400 MHz, $CDCl_3$) δ 8.88 (s, 1H), 8.65 (d, J = 8.2 Hz, 1H), 7.72 – 7.68 (m, 1H), 7.14 – 7.09 (m, 2H), 4.02 – 3.93 (m, 1H), 2.00 – 1.96 (m, 2H), 1.80 – 1.60 (m, 4H), 1.48 – 1.25 (m, 4H); ^{13}C NMR (101 MHz, $CDCl_3$) δ 167.0 (d, J = 258.8 Hz), 161.0, 160.1, 155.7 (d, J = 13.3 Hz), 147.4, 131.6 (d, J = 10.9 Hz), 117.6 (d, J = 2.9 Hz), 115.4 (d, J = 2.8 Hz), 113.8 (d, J = 23.3

Hz), 104.4 (d, J = 25.9 Hz), 48.5, 32.7 × 2, 25.5, 24.6 × 2; HRMS (ESI) calcd for $C_{16}H_{17}O_3NF$ ([M + H]$^+$) 290.1187, found 290.1179.

2.1.2.17. N-cycloheptyl-7-fluoro-2-oxo-2H-chromene-3-carboxamide ***(B8)***. Yield: 69 %, yellow solid, mp 190–192 °C; ^{1}H NMR (400 MHz, $CDCl_3$) δ 8.87 (s, 1H), 8.71 (d, J = 8.0 Hz, 1H), 7.71 – 7.68 (m, 1H), 7.20 – 7.03 (m, 2H), 4.20 – 4.11 (m, 1H), 2.02 – 1.97 (m, 2H), 1.71 – 1.54 (m, 10*H*); ^{13}C NMR (101 MHz, $CDCl_3$) δ 167.0 (d, J = 258.7 Hz), 161.0, 159.9, 155.7 (d, J = 13.2 Hz), 147.4, 131.5 (d, J = 10.7 Hz), 117.7 (d, J = 3.0 Hz), 115.5 (d, J = 2.8 Hz), 113.8 (d, J = 23.1 Hz), 104.4 (d, J = 25.9 Hz), 50.8, 34.7 × 2, 28.0 × 2, 24.1 × 2; HRMS (ESI) calcd for $C_{17}H_{19}O_3NF$ ([M + H]$^+$) 304.1343, found 304.1336.

2.1.2.18. 7-fluoro-2-oxo-N-o-tolyl-2H-chromene-3-carboxamide ***(B9)***. Yield: 71 %, white solid, mp 263–265 °C; ^{1}H NMR (400 MHz, $CDCl_3$) δ 10.66 (s, 1H), 9.02 (s, 1H), 8.23 (d, J = 8.1 Hz, 1H), 7.75 (t, J = 7.2 Hz, 1H), 7.28 – 7.08 (m, 5H), 2.42 (s, 3H); ^{13}C NMR (101 MHz, $CDCl_3$) δ 167.3 (d, J = 259.6 Hz), 161.6, 159.1, 155.8 (d, J = 13.6 Hz), 148.3, 136.0, 131.8 (d, J = 10.9 Hz), 130.5, 128.6, 126.7, 125.0, 121.9, 117.7 (d, J = 3.0 Hz), 115.5 (d, J = 2.2 Hz), 114.1 (d, J = 23.2 Hz), 104.6 (d, J = 25.9 Hz), 18.0; HRMS (ESI) calcd for $C_{17}H_{13}O_3NF$ ([M + H]$^+$) 298.0874, found 298.0867.

2.1.2.19. 7-fluoro-2-oxo-N-m-tolyl-2H-chromene-3-carboxamide ***(B10)***. Yield: 76 %, white solid, mp 222–224 °C; ^{1}H NMR (400 MHz, $CDCl_3$) δ 10.66 (s, 1H), 8.98 (s, 1H), 7.76 – 7.72 (m, 1H), 7.54 (d, J = 7.6 Hz, 2H), 7.26 (t, J = 8.0 Hz, 1H), 7.15 (t, J = 7.9 Hz, 2H), 6.98 (d, J = 7.5 Hz, 1H), 2.38 (s, 3H); ^{13}C NMR (101 MHz, $CDCl_3$) δ 167.3 (d, J = 259.6 Hz), 161.4, 159.0, 155.8 (d, J = 13.8 Hz), 148.2, 139.0, 137.4, 131.8 (d, J = 10.6 Hz), 128.9, 125.7, 121.1, 117.7, 117.6 (d, J = 3.3 Hz), 115.5 (d, J = 2.5 Hz), 114.1 (d, J = 23.3 Hz), 104.5 (d, J = 25.9 Hz), 21.4; HRMS (ESI) calcd for $C_{17}H_{13}O_3NF$ ([M + H]$^+$) 298.0874, found 298.0868.

2.1.2.20. N-(3,4-dimethylphenyl)-7-fluoro-2-oxo-2H-chromene-3-carboxamide ***(B11)***. Yield: 69 %, yellow solid, mp 200–202 °C; ^{1}H NMR (400 MHz, $CDCl_3$) δ 10.59 (s, 1H), 8.96 (s, 1H), 7.74 – 7.70 (m, 1H), 7.47 (d, J = 6.7 Hz, 2H), 7.17 – 7.10 (m, 3H), 2.28 (s, 3H), 2.24 (s, 3H); ^{13}C NMR (101 MHz, $CDCl_3$) δ 167.3 (d, J = 259.3 Hz), 161.4, 158.9, 155.8 (d, J = 13.5 Hz), 148.0, 137.3, 135.2, 133.3, 131.8 (d, J = 10.9 Hz), 130.0, 121.8, 118.0, 117.6 (d, J = 2.9 Hz), 115.5 (d, J = 2.1 Hz), 114.1 (d, J = 23.0 Hz), 104.5 (d, J = 25.8 Hz), 19.8, 19.2; HRMS (ESI) calcd for $C_{18}H_{15}O_3NF$ ([M + H]$^+$) 312.1030, found 312.1024.

2.1.2.21. N-(2,5-dimethylphenyl)-7-fluoro-2-oxo-2H-chromene-3-carboxamide ***(B12)***. Yield: 85 %, yellow solid, mp 216–218 °C; ^{1}H NMR (400 MHz, $CDCl_3$) δ 10.60 (s, 1H), 9.00 (s, 1H), 8.05 (s, 1H), 7.76 – 7.72 (m, 1H), 7.17 – 7.09 (m, 3H), 6.91 (d, J = 7.4 Hz, 1H), 2.36 (s, 6H); ^{13}C NMR (101 MHz, $CDCl_3$) δ 167.3 (d, J = 259.6 Hz), 161.5, 159.0, 155.8 (d, J = 13.7 Hz), 148.2, 136.4, 135.7, 131.8 (d, J = 10.8 Hz), 130.2, 125.8, 125.5, 122.5, 117.7 (d, J = 3.3 Hz), 115.5 (d, J = 2.8 Hz), 114.1 (d, J = 22.9 Hz), 104.5 (d, J = 26.0 Hz), 21.2, 17.6; HRMS (ESI) calcd for $C_{18}H_{15}O_3NF$ ([M + H]$^+$) 312.1030, found 312.1023.

2.1.2.22. N-(2,6-dimethylphenyl)-7-fluoro-2-oxo-2H-chromene-3-carboxamide ***(B13)***. Yield: 84 %, yellow solid, mp 215–217 °C; ^{1}H NMR (400 MHz, $CDCl_3$) δ 10.06 (s, 1H), 9.01 (s, 1H), 7.74 – 7.71 (m, 1H), 7.19 – 7.10 (m, 5H), 2.28 (s, 6H); ^{13}C NMR (101 MHz, $CDCl_3$) δ 167.3 (d, J = 259.6 Hz), 161.5, 159.5, 155.9 (d, J = 13.6 Hz), 148.5, 135.0 × 2, 133.7, 131.8 (d, J = 10.8 Hz), 128.2 × 2, 127.4, 117.3 (d, J = 2.9 Hz), 115.5 (d, J = 2.3 Hz), 114.1 (d, J = 23.2 Hz), 104.5 (d, J = 25.9 Hz), 18.6 × 2; HRMS (ESI) calcd for $C_{18}H_{15}O_3NF$ ([M + H]$^+$) 312.1030, found 312.1024.

2.1.2.23. 7-fluoro-N-(3-methoxyphenyl)-2-oxo-2H-chromene-3-carboxamide ***(B14)***. Yield: 88 %, white solid, mp 226–228 °C; ^{1}H NMR (400 MHz, $CDCl_3$) δ 11.18 (s, 1H), 8.97 (s, 1H), 8.52 (d, J = 8.1 Hz, 1H), 7.74 – 7.67 (m, 1H), 7.19 – 7.09 (m, 3H), 7.00 (t, J = 7.6 Hz, 1H), 6.94 (d, J = 8.0 Hz, 1H), 3.97 (s, 3H); ^{13}C NMR (101 MHz, $CDCl_3$) δ 167.2 (d, J = 253.5 Hz), 161.0, 158.9, 155.8 (d, J = 13.4 Hz), 149.1, 147.9, 131.7 (d, J = 10.9 Hz), 127.6, 124.6, 120.9, 120.6, 117.9 (d, J = 2.9 Hz), 115.5 (d, J = 2.6 Hz), 114.0 (d, J = 23.2 Hz), 110.2, 104.5 (d, J = 25.7 Hz), 55.9; HRMS (ESI) calcd for $C_{17}H_{13}O_4NF$ ([M + H]$^+$) 314.0823, found 314.0816.

2.1.2.24. N-ethyl-8-fluoro-2-oxo-2H-chromene-3-carboxamide ***(C1)***. Yield: 60 %, white solid, mp 191–192 °C; ^{1}H NMR (400 MHz, $CDCl_3$) δ 8.92 (s, 1H), 8.70 (s, 1H), 7.49 – 7.41 (m, 2H), 7.35 – 7.30 (m, 1H), 3.51 (p, J = 6.9 Hz, 2H), 1.27 (t, J = 7.3 Hz, 3H); ^{13}C NMR (101 MHz, $CDCl_3$) δ 160.8, 160.1, 150.3 (d, J = 254.7 Hz), 147.6 (d, J = 2.9 Hz), 142.5 (d, J = 11.2 Hz), 125.1 (d, J = 6.6 Hz), 124.8 (d, J = 4.2 Hz), 120.4, 120.1 (d, J = 17.1 Hz), 119.4, 34.8, 14.6; HRMS (ESI) calcd for $C_{12}H_{11}O_3NF$ ([M + H]$^+$) 236.0717, found 236.0712.

2.1.2.25. 8-fluoro-2-oxo-N-propyl-2H-chromene-3-carboxamide ***(C2)***. Yield: 55 %, white solid, mp 185–186 °C; ^{1}H NMR (400 MHz, $CDCl_3$) δ 8.92 (s, 1H), 8.75 (s, 1H), 7.49 (d, J = 7.8 Hz, 1H), 7.47 – 7.41 (m, 1H), 7.33 (td, J = 8.0, 4.5 Hz, 1H), 3.47 – 3.41 (m, 2H), 1.71 – 1.62 (m, 2H), 1.00 (t, J = 7.4 Hz, 3H); ^{13}C NMR (101 MHz, $CDCl_3$) δ 160.9, 160.1, 150.3 (d, J = 254.6 Hz), 147.6 (d, J = 2.9 Hz), 142.5 (d, J = 11.6 Hz), 125.1 (d, J = 6.9 Hz), 124.8 (d, J = 4.2 Hz), 120.4, 120.1 (d, J = 16.7 Hz), 119.5, 41.6, 22.6, 11.4; HRMS (ESI) calcd for $C_{13}H_{13}O_3NF$ ([M + H]$^+$) 250.0874, found 250.0869.

2.1.2.26. N-butyl-8-fluoro-2-oxo-2H-chromene-3-carboxamide ***(C3)***. Yield: 77 %, white solid, mp 148–149 °C; ^{1}H NMR (400 MHz, $CDCl_3$) δ 8.92 (d, J = 1.6 Hz, 1H), 8.73 (s, 1H), 7.48 (d, J = 7.8 Hz, 1H), 7.46 – 7.41 (m, 1H), 7.33 (td, J = 8.0, 4.5 Hz, 1H), 3.51 – 3.43 (m, 2H), 1.63 (p, J = 7.6 Hz, 2H), 1.45 – 1.38 (m, 2H), 0.97 (t, J = 7.3 Hz, 3H); ^{13}C NMR (101 MHz, $CDCl_3$) δ 160.9, 160.1, 150.3 (d, J = 254.6 Hz), 147.6 (d, J = 2.8 Hz), 142.5 (d, J = 11.6 Hz), 125.1 (d, J = 6.7 Hz), 124.8 (d, J = 3.8 Hz), 120.4, 120.1 (d, J = 17.3 Hz), 119.5, 39.7, 31.4, 20.1, 13.7; HRMS (ESI) calcd for $C_{14}H_{15}O_3NF$ ([M + H]$^+$) 264.1030, found 264.1024.

2.1.2.27. 8-fluoro-N-hexyl-2-oxo-2H-chromene-3-carboxamide ***(C4)***. Yield: 66 %, yellow solid, mp 110–111 °C; ^{1}H NMR (400 MHz, $CDCl_3$) δ 8.92 (d, J = 1.6 Hz, 1H), 8.73 (s, 1H), 7.48 (d, J = 7.8 Hz, 1H), 7.46 – 7.41 (m, 1H), 7.32 (td, J = 8.0, 4.5 Hz, 1H), 3.48 – 3.42 (m, 2H), 1.63 (q, J = 7.6 Hz, 2H), 1.43 – 1.30 (m, 6H), 0.89 (t, J = 7.5 Hz, 3H); ^{13}C NMR (101 MHz, $CDCl_3$) δ 160.8, 160.1, 150.4 (d, J = 254.9 Hz), 147.6 (d, J = 2.7 Hz), 142.5 (d, J = 11.2 Hz), 125.1 (d, J = 6.6 Hz), 124.8 (d, J = 3.7 Hz), 120.4, 120.1 (d, J = 17.0 Hz), 119.5, 40.0, 31.4, 29.2, 26.6, 22.5, 13.9; HRMS (ESI) calcd for $C_{16}H_{19}O_3NF$ ([M + H]$^+$) 292.1343, found 292.1337.

2.1.2.28. 8-fluoro-2-oxo-N-(pentan-3-yl)–2H-chromene-3-carboxamide ***(C5)***. Yield: 89 %, yellow solid, mp 115–116 °C; ^{1}H NMR (400 MHz, $CDCl_3$) δ 8.92 (d, J = 1.6 Hz, 1H), 8.53 (d, J = 8.8 Hz, 1H), 7.48 (d, J = 7.8 Hz, 1H), 7.46 – 7.41 (m, 1H), 7.32 (td, J = 8.0, 4.5 Hz, 1H), 4.04 – 3.95 (m, 1H), 1.72 – 1.61 (m, 2H), 1.60 – 1.51 (m, 2H), 0.96 (t, J = 7.5 Hz, 6H); ^{13}C NMR (101 MHz, $CDCl_3$) δ 160.6, 160.2, 150.3 (d, J = 254.7 Hz), 147.6 (d, J = 2.8 Hz), 142.5 (d, J = 11.6 Hz), 125.1 (d, J = 6.6 Hz), 124.8 (d, J = 3.8 Hz), 120.5, 120.0 (d, J = 16.8 Hz), 119.6, 52.7, 27.2 × 2, 10.2 × 2; HRMS (ESI) calcd for $C_{15}H_{17}O_3NF$ ([M + H]$^+$) 278.1187, found 278.1179.

2.1.2.29. N-cyclopropyl-8-fluoro-2-oxo-2H-chromene-3-carboxamide ***(C6)***. Yield: 80 %, white solid, mp 204–205 °C; ^{1}H NMR (400 MHz, $CDCl_3$) δ 8.93 (d, J = 1.6 Hz, 1H), 8.73 (s, 1H), 7.49 (d, J = 7.7 Hz, 1H), 7.46 – 7.41(m, 1H), 7.33 (td, J = 8.0, 4.5 Hz, 1H), 2.99 – 2.93 (m, 1H), 0.91 – 0.86 (m, 2H), 0.69 – 0.64 (m, 2H); ^{13}C NMR (101 MHz, $CDCl_3$) δ

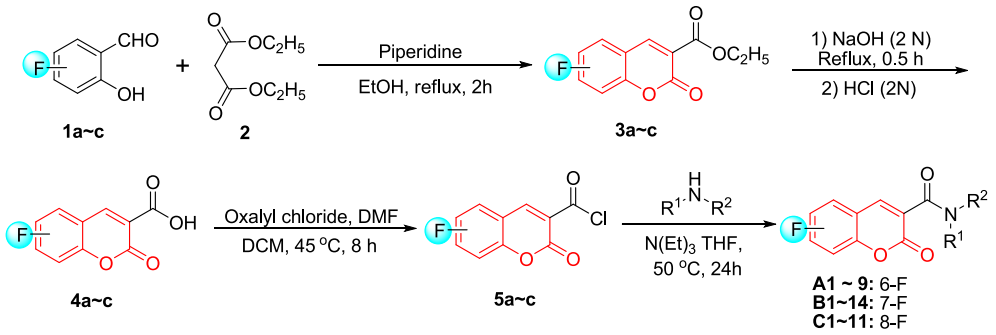

Scheme 1. Synthetic route for coumarin amide derivatives bearing fluorine.

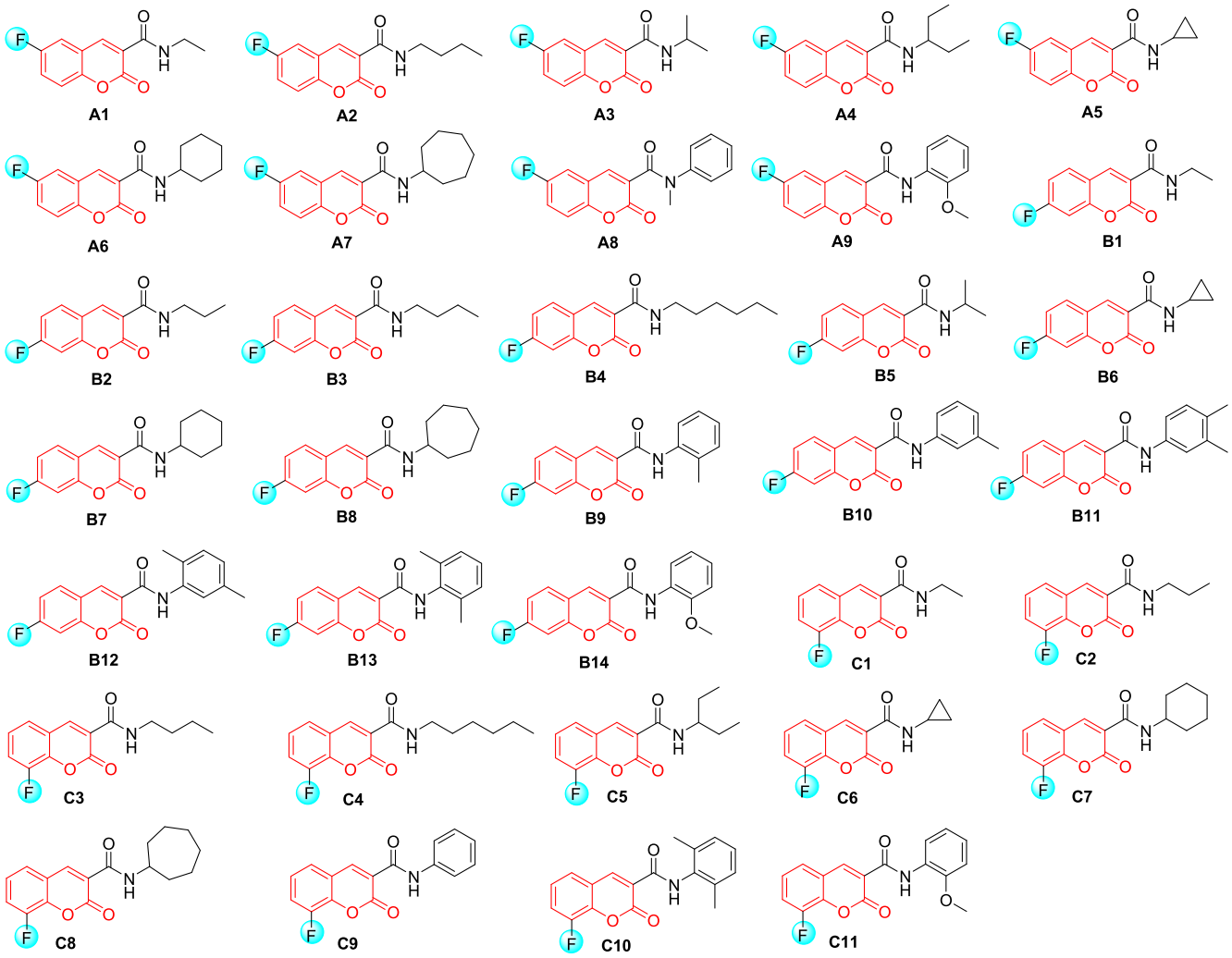

Fig. 2. Chemical Structures of compounds **A1-9**, **B1-14**, **C1-11**.

162.3, 160.0, 150.3 (d, J = 255.1 Hz), 147.5 (d, J = 2.8 Hz), 142.5 (d, J = 11.6 Hz), 125.2 (d, J = 6.7 Hz), 124.9 (d, J = 4.2 Hz), 120.4, 120.2 (d, J = 17.0 Hz), 119.2, 23.0, 6.6 × 2; HRMS (ESI) calcd for $C_{13}H_{11}O_3NF$ ([M + H]$^+$) 248.0717, found 248.0710.

2.1.2.30. N-cyclohexyl-8-fluoro-2-oxo-2H-chromene-3-carboxamide ***(C7)***. Yield: 69 %, yellow solid, mp 173–174 °C; ^{1}H NMR (400 MHz, $CDCl_3$) δ 8.91 (d, J = 1.6 Hz, 1H), 8.67 (d, J = 8.0 Hz, 1H), 7.48 (d, J = 7.8 Hz, 1H), 7.46 – 7.40 (m, 1H), 7.32 (td, J = 8.0, 4.5 Hz, 1H), 4.02 – 3.93 (m, 1H), 2.01 – 1.97 (m, 2H), 1.79 – 1.73 (m, 2H), 1.68 – 1.60 (m, 1H), 1.47 – 1.22 (m, 5H); ^{13}C NMR (101 MHz, $CDCl_3$) δ 160.1, 159.8, 150.3 (d, J = 254.8 Hz), 147.5 (d, J = 2.4 Hz), 142.5 (d, J = 11.6 Hz), 125.1 (d, J = 6.7 Hz), 124.8 (d, J = 4.2 Hz), 120.5, 120.0 (d, J = 17.0 Hz), 119.7, 48.7, 32.7 × 2, 25.5, 24.6 × 2; HRMS (ESI) calcd for $C_{16}H_{17}O_3NF$ ([M + H]$^+$) 290.1187, found 290.1180.

2.1.2.31. N-cycloheptyl-8-fluoro-2-oxo-2H-chromene-3-carboxamide ***(C8)***. Yield: 73 %, yellow solid, mp 138–139 °C; ^{1}H NMR (400 MHz, $CDCl_3$) δ 8.90 (d, J = 1.6 Hz, 1H), 8.73 (d, J = 8.0 Hz, 1H), 7.48 (d, J = 7.9 Hz, 1H), 7.45 – 7.40 (m, 1H), 7.32 (td, J = 8.0, 4.4 Hz, 1H), 4.21 –

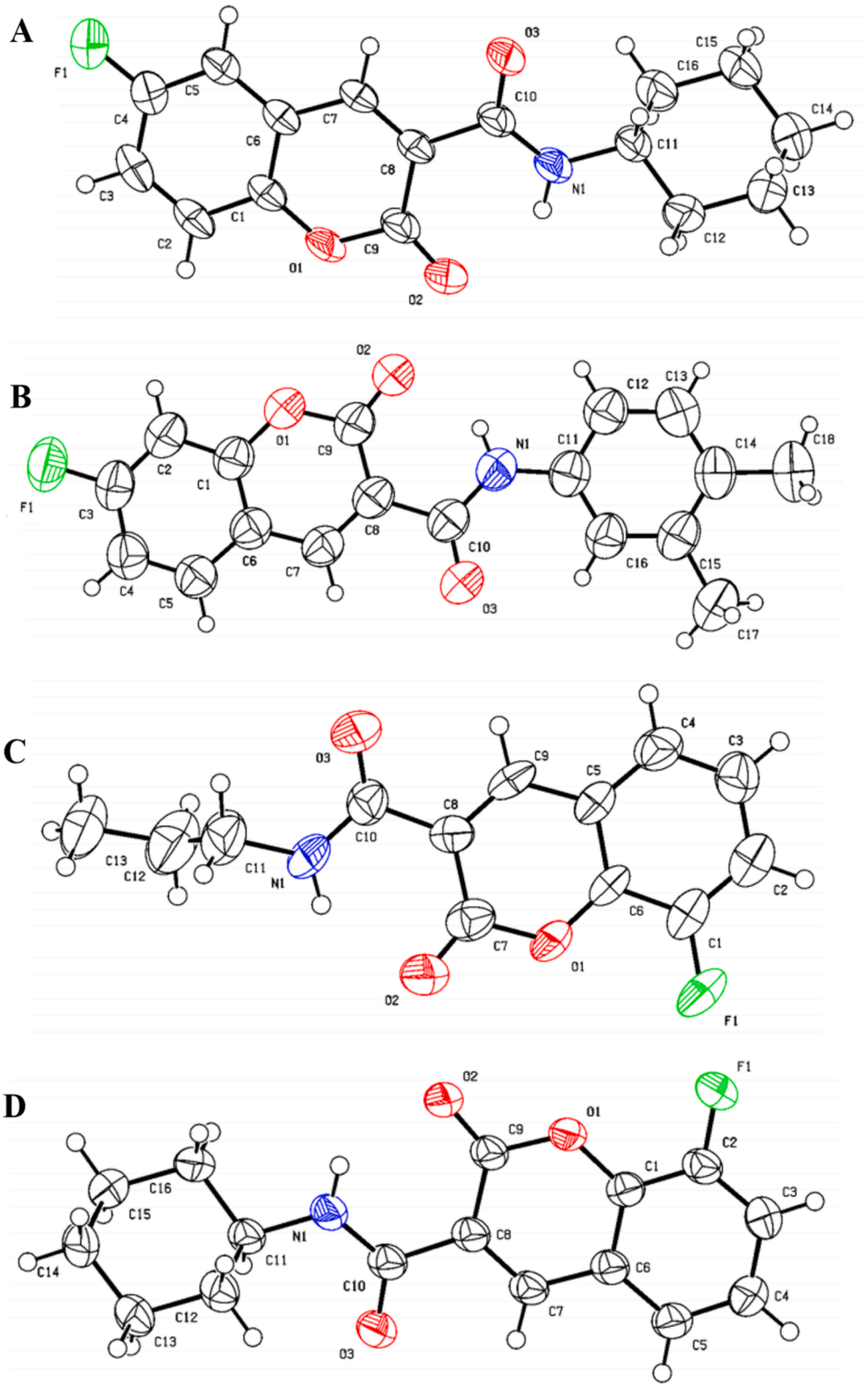

Fig. 3. X-ray crystallographic structures of **A6** (A), **B11** (B), **C2** (C) and **C7** (D).

4.11 (m, 1H), 2.05 – 1.96 (m, 2H), 1.71 – 1.55 (m, 10*H*); ^{13}C NMR (101 MHz, $CDCl_3$) δ 160.1, 159.6, 150.3 (d, J = 255.0 Hz), 147.4 (d, J = 2.7 Hz), 142.5 (d, J = 11.7 Hz), 125.1 (d, J = 6.6 Hz), 124.8 (d, J = 4.1 Hz), 120.5, 120.0 (d, J = 17.4 Hz), 119.7, 50.9, 34.7 × 2, 27.9 × 2, 24.1 × 2; HRMS (ESI) calcd for $C_{17}H_{19}O_3NF$ ([M + H]$^+$) 304.1343, found 304.1336.

2.1.2.32. 8-fluoro-2-oxo-N-phenyl-2H-chromene-3-carboxamide ***(C9)***. Yield: 73 %, white solid, mp 282–283 °C; ^{1}H NMR (400 MHz, $CDCl_3$) δ 10.97 (s, 1H), 9.20 (s, 1H), 7.64 – 7.53 (m, 4H), 7.48 – 7.39 (m, 3H), 7.29 (t, J = 7.4 Hz, 1H); ^{13}C NMR (101 MHz, $CDCl_3$) δ 160.4, 160.0, 150.4, 150.3 (d, J = 255.4 Hz), 142.4 (d, J = 11.6 Hz), 135.6, 129.3 × 2, 126.7, 126.0 (d, J = 6.4 Hz), 125.6 (d, J = 3.9 Hz), 122.1, 122.0 × 2,

Table 1
Antifungal activity of target compounds against phytopathogens at 50 μg/mL.

Compounds	Antifungal activities (inhibition % ± SE)[a,b,c]				
	AB	AA	CG	PG	FV
A1	43.2 ± 1.8	44.5 ± 0.0	46.7 ± 0.0	36.7 ± 2.0	41.1 ± 1.3
A2	27.9 ± 2.0	40.7 ± 3.5	34.7 ± 2.4	36.9 ± 1.7	24.4 ± 1.7
A3	46.5 ± 2.0	53.5 ± 2.3	33.3 ± 4.2	37.9 ± 1.7	24.4 ± 3.4
A4	55.8 ± 2.0	70.9 ± 1.8	41.7 ± 1.3	58.3 ± 1.7	26.4 ± 0.0
A5	48.8 ± 2.0	52.3 ± 4.0	30.6 ± 2.4	43.7 ± 1.7	21.4 ± 1.7
A6	34.9 ± 5.3	34.9 ± 5.3	31.9 ± 2.4	32.0 ± 1.7	21.4 ± 1.7
A7	50.0 ± 2.0	67.4 ± 2.0	29.2 ± 0.0	40.8 ± 1.7	23.4 ± 4.6
A8	20.9 ± 5.3	41.9 ± 2.0	18.1 ± 2.4	38.8 ± 0.0	24.4 ± 1.7
A9	17.9 ± 2.0	33.3 ± 0.0	24.6 ± 0.0	34.5 ± 2.0	34.5 ± 1.7
B1	31.5 ± 0.0	34.5 ± 0.0	35.8 ± 0.0	37.9 ± 2.0	31.1 ± 0.0
B2	61.6 ± 1.8	67.3 ± 3.9	65.3 ± 0.0	44.7 ± 0.0	42.3 ± 3.1
B3	46.5 ± 1.5	64.0 ± 1.8	55.6 ± 2.0	50.5 ± 2.4	37.3 ± 0.0
B4	24.4 ± 3.2	37.2 ± 0.0	22.2 ± 2.0	41.7 ± 0.0	25.4 ± 3.1
B5	53.4 ± 0.0	45.6 ± 1.2	43.4 ± 2.0	48.9 ± 0.0	38.0 ± 0.0
B6	51.2 ± 3.5	57.0 ± 3.4	45.8 ± 2.0	45.6 ± 0.0	27.4 ± 0.0
B7	36.0 ± 5.3	43.0 ± 4.0	47.2 ± 4.8	45.6 ± 1.7	31.3 ± 5.2
B8	43.0 ± 1.9	46.5 ± 0.0	45.8 ± 1.9	42.7 ± 1.7	37.3 ± 2.8
B9	29.6 ± 5.3	39.5 ± 5.3	27.8 ± 2.4	46.6 ± 4.4	25.4 ± 0.0
B10	31.4 ± 0.0	36.0 ± 0.0	29.2 ± 1.6	39.8 ± 1.7	25.4 ± 0.0
B11	32.6 ± 2.4	32.6 ± 2.0	33.3 ± 0.0	41.7 ± 0.0	25.4 ± 0.0
B12	32.6 ± 2.0	48.8 ± 0.0	31.9 ± 0.0	35.0 ± 0.0	25.4 ± 2.0
B13	39.5 ± 2.3	53.5 ± 2.0	29.2 ± 0.0	56.3 ± 0.0	25.4 ± 0.0
B14	33.7 ± 1.0	46.5 ± 3.8	31.9 ± 3.7	50.0 ± 2.0	29.0 ± 0.0
C1	40.4 ± 1.6	29.4 ± 1.3	30.2 ± 0.9	40.2 ± 4.2	30.3 ± 5.4
C2	38.4 ± 0.0	53.5 ± 2.0	65.3 ± 1.3	44.7 ± 0.0	25.4 ± 1.5
C3	45.3 ± 2.0	60.7 ± 2.0	66.7 ± 1.7	45.6 ± 1.7	29.4 ± 1.7
C4	46.5 ± 2.0	46.5 ± 2.0	41.7 ± 0.0	46.6 ± 1.7	41.3 ± 1.7
C5	54.7 ± 3.5	88.4 ± 2.0	86.1 ± 2.4	59.2 ± 2.9	46.3 ± 3.0
C6	47.7 ± 3.5	55.8 ± 5.3	75.0 ± 4.2	46.6 ± 1.7	33.3 ± 1.7
C7	46.5 ± 3.3	51.9 ± 0.0	44.4 ± 0.0	39.9 ± 0.0	46.3 ± 0.0
C8	46.5 ± 2.0	58.1 ± 3.5	59.7 ± 9.6	44.7 ± 2.9	38.3 ± 3.4
C9	36.0 ± 5.3	38.4 ± 5.3	22.2 ± 2.4	34.0 ± 3.4	28.4 ± 5.2
C10	34.9 ± 1.8	52.3 ± 2.2	23.6 ± 0.0	25.4 ± 2.0	26.4 ± 2.0
C11	31.4 ± 1.0	47.7 ± 3.5	29.2 ± 2.0	40.8 ± 3.4	25.4 ± 1.7
Kre	63.1 ± 2.5	64.3 ± 0.0	53.0 ± 8.1	53.0 ± 0.7	58.3 ± 0.0

[a] AB: *Alternaria brassicae*, AA: *Alternaria alternata*, CG: *Colletotrichum gloeosporioides*, PG: *Pyricularia grisea,* FV: *Fusarium oxysporium f. sp.vasinfectum.*
[b] Values are the mean ± SE of three replicates.
[c] Kre: Kresoxim-methyl.

Table 2
EC_{50} values of compound **C5** against phytopathogens [a,b,c].

Fungi	Compound	Regression equation	R^2	EC_{50} (μg/mL)	95 % CI (μg/mL)
AB	**C5**	$y = 0.8040x + 3.7436$	0.9528	36.5*	30.7–44.6
	Kre	$y = 0.4424x + 4.4902$	0.9527	14.2	9.8–20.4
AA	**C5**	$y = 1.5709x + 3.3365$	0.9526	11.5*	6.5–17.5
	Kre	$y = 2.3629x + 2.1090$	0.9826	15.5	14.1–17.0
CG	**C5**	$y = 1.7678x + 2.7826$	0.9448	18.0*	12.1–24.5
	Kre	$y = 0.3288x + 4.5625$	0.9702	21.5	20.3–25.2
PG	**C5**	$y = 0.8422x + 3.7122$	0.9314	33.8*	28.6–40.5
	Kre	$y = 0.7208x + 3.5630$	0.9955	53.7	49.7–58.4

Significant difference between the treatment group and Kre group (* $p < 0.05$).
[a] AB: *Alternaria brassicae*, AA: *Alternaria alternata*, CG: *Colletotrichum gloeosporioides*, PG: *Pyricularia grisea*.
[b] 50% Effective concentration (EC_{50}): concentration of compound that inhibits the fungi growth; 95% CI means 95% confidence interval of EC_{50}, values are mean of three replicates.
[c] Kre: Kresoxim-methyl.

121.4 (d, $J = 17.3$ Hz), 120.1; HRMS (ESI) calcd for $C_{16}H_{11}O_3NF$ ($[M + H]^+$) 284.0717, found 284.0712.

*2.1.2.33. N-(2,6-dimethylphenyl)-8-fluoro-2-oxo-2H-chromene-3-carboxamide **(C10)**.* Yield: 87 %, white solid, mp 247–248 °C; ^1H NMR (400 MHz, $CDCl_3$) δ 10.08 (s, 1H), 9.04 (d, $J = 1.6$ Hz, 1H), 7.52 – 7.44 (m, 2H), 7.35 (td, $J = 8.0$, 4.4 Hz, 1H), 7.17 – 7.10 (m, 3H), 2.29 (s, 6H); ^{13}C NMR (101 MHz, $CDCl_3$) δ 160.6, 159.2, 150.4 (d, $J = 255.2$ Hz), 148.5, 142.7 (d, $J = 11.6$ Hz), 135.0, 133.6 × 2, 128.2 × 2, 127.4, 125.3 (d, $J = 6.5$ Hz), 125.0 (d, $J = 4.2$ Hz), 120.5, 120.4 (d, $J = 14.1$ Hz), 119.4, 18.5 × 2; HRMS (ESI) calcd for $C_{18}H_{15}O_3NF$ ($[M + H]^+$) 312.1030, found 312.1022.

*2.1.2.34. 8-fluoro-N-(2-methoxyphenyl)-2-oxo-2H-chromene-3-carboxamide **(C11)**.* Yield: 76 %, white solid, mp 240–241 °C; ^1H NMR (400 MHz, $CDCl_3$) δ 11.22 (s, 1H), 9.00 (d, $J = 1.6$ Hz, 1H), 8.52 (dd, $J = 8.0$, 1.6 Hz, 1H), 7.51 (d, $J = 7.8$ Hz, 1H), 7.48 – 7.42 (m, 1H), 7.34 (td, $J = 8.0$, 4.5 Hz, 1H), 7.12 (td, $J = 7.8$, 1.6 Hz, 1H), 7.00 (td, $J = 7.8$, 1.4 Hz, 1H), 6.94 (dd, $J = 8.2$, 1.4 Hz, 1H), 3.97 (s, 3H); ^{13}C NMR (101 MHz, $CDCl_3$) δ 160.1, 158.6, 150.4 (d, $J = 254.8$ Hz), 149.1, 147.9 (d, $J = 11.4$ Hz), 142.6 (d, $J = 11.4$ Hz), 127.5, 125.2 (d, $J = 6.4$ Hz), 124.9 (d, $J = 3.9$ Hz), 124.7, 120.9, 120.6, 120.4, 120.3 (d, $J = 17.0$ Hz), 119.6, 110.3, 56.0; HRMS (ESI) calcd for $C_{17}H_{13}O_4NF$ ($[M + H]^+$) 314.0823, found 314.0816.

2.2. Antifungal assay

In vitro evaluations were conducted on compounds **A1 ~ 9**, **B1 ~ 14,** and **C1 ~ 11** to assess their impact on the growth of phytopathogenic fungi by inhibiting mycelial growth. Five phytopathogenic fungi, including *Alternaria brassicae* (AB), *Alternaria alternata* (AA), *Colletotrichum gloeosporioides* (CG), *Pyricularia grisea* (PG), *Fusarium oxysporium f. sp.vasinfectum* (FV) were used for the assays. The dissolved compounds in acetone were combined with the PDA at 50 μg/mL before being transferred to sterilized Petri dishes. Acetone served as blank controls, and kresoxim-methyl, a commercial fungicide, used as the positive

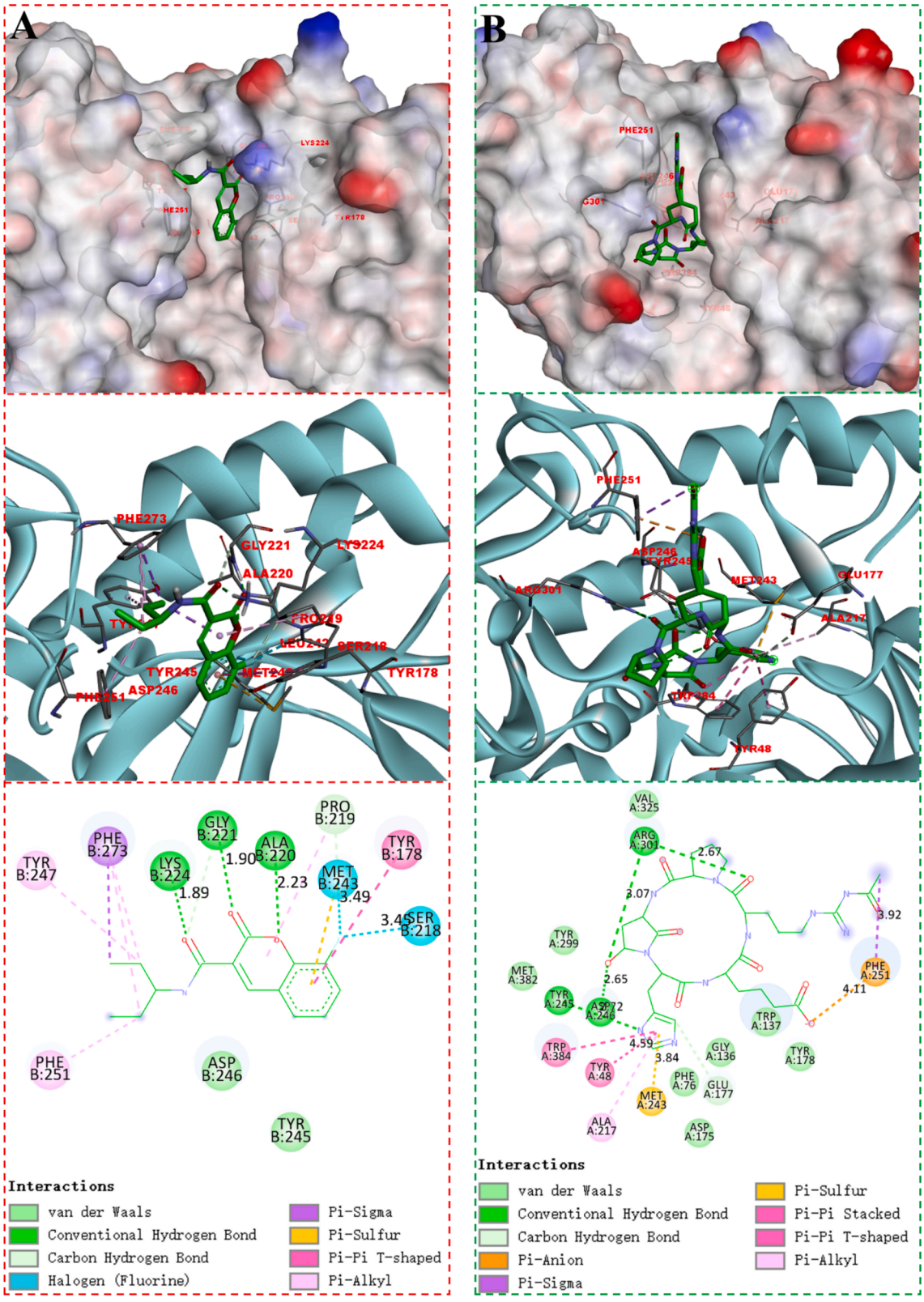

Fig. 4. Molecular models of **C5** (A) and argadin (B) binding to chitinase.

control. Mycelia disks measuring 4 mm in diameter were inoculated onto PDA Petri dishes and incubated at 25 °C for a period of 4 days. Three replicates were performed for every treatment, measuring the radial growth of fungal colonies and analyzing the data statistically. Subsequently, the inhibition rates (%) versus seven concentrations of some compounds and kresoxim-methyl were obtained, and the median effective concentration (EC_{50}) values were calculated.

Table 3
The anticancer activities of target compounds against human cancer cells at 100 μmol/L.

Compound	Growth Inhibition Rate (%)[a]		
	HeLa	HePG-2	HCT116
A1	48.50 ± 5.00	44.69 ± 0.17	40.02 ± 2.03
A2	51.98 ± 5.49	53.02 ± 5.11	41.91 ± 3.16
A3	43.13 ± 4.41	33.51 ± 0.20	NA
A4	90.28 ± 0.54	73.58 ± 1.34	76.01 ± 1.27
A5	48.82 ± 4.17	45.72 ± 3.71	NA
A6	45.99 ± 4.47	45.69 ± 0.61	18.05 ± 5.36
A7	46.31 ± 1.14	50.14 ± 4.34	22.9 ± 4.58
A8	32.23 ± 3.32	35.88 ± 4.05	16.18 ± 0.97
A9	61.48 ± 3.08	21.77 ± 4.97	NA
B1	29.80 ± 2.33	19.83 ± 1.52	27.55 ± 4.01
B2	50.42 ± 4.46	45.00 ± 3.11	39.25 ± 3.51
B3	53.57 ± 5.85	48.91 ± 5.08	37.32 ± 3.19
B4	38.30 ± 4.57	41.64 ± 3.76	16.19 ± 2.12
B5	26.08 ± 4.64	14.75 ± 1.44	20.97 ± 1.72
B6	12.00 ± 0.32	11.66 ± 0.8	15.57 ± 2.35
B7	38.27 ± 8.93	38.54 ± 5.41	18.38 ± 0.71
B8	33.07 ± 2.93	16.07 ± 0.04	15.65 ± 2.34
B9	22.27 ± 3.50	11.00 ± 2.09	5.43 ± 3.29
B10	29.88 ± 1.84	22.38 ± 3.28	15.73 ± 1.50
B11	43.62 ± 4.72	40.48 ± 3.10	31.90 ± 4.53
B12	27.58 ± 4.21	14.79 ± 2.88	18.60 ± 1.16
B13	17.59 ± 0.87	8.74 ± 2.11	5.28 ± 1.90
B14	46.19 ± 4.66	37.66 ± 3.70	35.00 ± 0.84
C1	21.83 ± 2.73	12.91 ± 1.61	NA
C2	19.90 ± 0.15	11.13 ± 1.37	NA
C3	21.00 ± 1.69	11.31 ± 1.82	NA
C4	24.57 ± 4.62	17.65 ± 1.23	NA
C5	16.98 ± 2.17	11.69 ± 4.31	NA
C6	21.81 ± 2.21	15.99 ± 0.61	NA
C7	17.76 ± 1.79	14.02 ± 0.84	NA
C8	21.34 ± 2.68	25.76 ± 5.87	NA
C9	49.82 ± 3.29	30.59 ± 0.77	NA
C10	28.54 ± 1.40	31.35 ± 4.30	10.72 ± 3.46
C11	52.66 ± 1.90	46.68 ± 5.01	34.08 ± 3.16
5-Fu	85.00 ± 2.01	64.65 ± 0.62	92.36 ± 3.64

[b]NA means no action.
[a] The values given are means of three experiments.

2.3. Molecular docking studies

ChemDraw2019 was used to create a 2D structure of compound **C5**, which was saved as a cdx file. Next, the 3D structure of **C5** was optimized using the MM2 force field in Chem3D 2019. Chitinase's 3D configurations were obtained from the PDB repository (https://www.rcsb.org, PDB: 1W9U). Subsequently, the proteins of interest were brought into AutoDock Tools for the processes of adding hydrogen atoms, calculating charges, and combining non-polar hydrogens, with the final outcome being saved in PDBQT format. Ultimately, execute AutoDock Vina to perform molecular docking, then utilize Discovery studio for visualizing the outcomes.

2.4. Anticancer assay

Three human cancer cells, including HeLa, HePG-2, HCT116, and normal human cells (BEAS-2B) were used to determine the cytotoxic effects of the prepared compounds (**A1** ~ **9**, **B1** ~ **14**, **C1** ~ **11**), and CCK-8 assay was used to assess the impact on growth. Cells were placed in 96-well plates and exposed to the compounds at a concentration of 100 μmol/L for 48 h in triplicate. Each well was treated with CCK-8 solution at a concentration of 20 %, followed by incubation for 1 h and measurement using spectrophotometry at 450 nm. As a positive control, 5-fluorouracil (**5-FU**) was also used in identical conditions. The additional IC_{50} values for certain compounds was also tested. Each experiment was conducted thrice.

2.5. Cell cycle arrest assay

HeLa cells (2×10^6/well) were seeded in 6-well plates and incubated overnight, and then exposed to **A4** (0, 4, 8, 16 μM) for 48 h. Afterward, PBS was rinsed over the cells and trypsin was added. After centrifugation, the liquid above the sediment was discarded and the remaining material was soaked in 70 % ethanol overnight. The cells were rinsed with PBS two times and then placed in a staining buffer with 190 μL volume, which included propidium iodide (1 mg/mL, 4 μL) and RNaseA (ribonuclease, 10 mg/mL, 4 μL), and Tritonx-100 (0.2 μL). Following a 20-minute staining period in darkness, the distribution of the cell cycle was analyzed with flow cytometry.

2.6. Cell apoptosis assay

The incubated HeLa cells (2×10^6/well) were exposed to **A4** (0, 4, 8, 16 μM) for 48 h. Following the incubation period, PBS was rinsed over the cells and trypsin was added. Then the resulting cell was tmixed with Annexin binding buffer. Subsequently, annexin V/FITC (5 μL) and PI (10 μL) were introduced to the cell suspension and allowed to incubate at appropriate temperature for 15 min. Afterward, flow cytometry underwent analysis the stained cells.

2.7. Data analyses

The formula used to calculate the inhibitory effects on these fungi in vitro is Inhibition rate (%) = (C-T) × 100/(C-4 mm), with C representing the diameter in the blank control group and T representing the diameter in the treatments. The cell Inhibition rate (%) = (OD1-OD2)/(OD1-OD3) × 100 %. The cell viability rate (%) = (OD2-OD3) / (OD1-OD3) × 100 %. with OD1, OD2,OD3 representing the negative control, experiment and blank group. GraphPad Prism 8 software (GraphPad, Inc., San Diego, CA) was used to conduct statistical analysis.

3. Results and discussion

3.1. Chemistry

As shown in Scheme 1, initially, primary coumarin-3-formyl chlorides **5a** ~ **c** were synthesized through a four-step process beginning with readily available salicylaldehydes. Salicylaldehydes **1a** ~ **c** were subjected to Knoevenagle condensation with diethyl malonate (**2**) in ethanol by a catalytic amount of piperidine, forming coumarin-3-carboxylates **3a** ~ **c**. Next, the ethyl esters underwent hydrolysis using a NaOH solution to produce coumarin-3-carboxylic acids **4a** ~ **c**, which reacted with oxalyl chloride to give the intermediates **5a** ~ **c**. At last, a series of coumarin amide derivatives bearing fluorine (**A1** ~ **9**, **B1** ~ **14**, **C1** ~ **11**) were prepared in 55 ~ 89 % yields by reaction of **5a** ~ **c** with different amines in the presence of triethylamine at 50 °C. Fig. 2 summarizes all the structures. The chemical structures of these derivatives were verified using ^{1}H NMR, ^{13}C NMR and HRMS spectrometry (see Supporting Information). Moreover, X-ray diffraction was used to identify the stereo structures of **A6**, **B11**, **C2** and **C7**, as shown in Fig. 3. The crystallographic data of these compounds were submitted to the CCDC under no. 2337042, 2337478, 2,337,043 and 2337044, respectively (see Supporting Information).

3.2. Antifungal activities

All the target compounds were screened their antifungal activities in vitro against five phytopathogenic fungi at 50 μg/mL using the mycelium linear growth rate method (Liu et al., 2022). Kresoxim-methyl (Kre) was used as positive control. As illustrated in Table 1, several compounds displayed significant inhibitory effects on specific fungi, which was consistent with the previous research findings that coumarin-3-carboxamide derivatives have good antibacterial activity (Yu et al.,

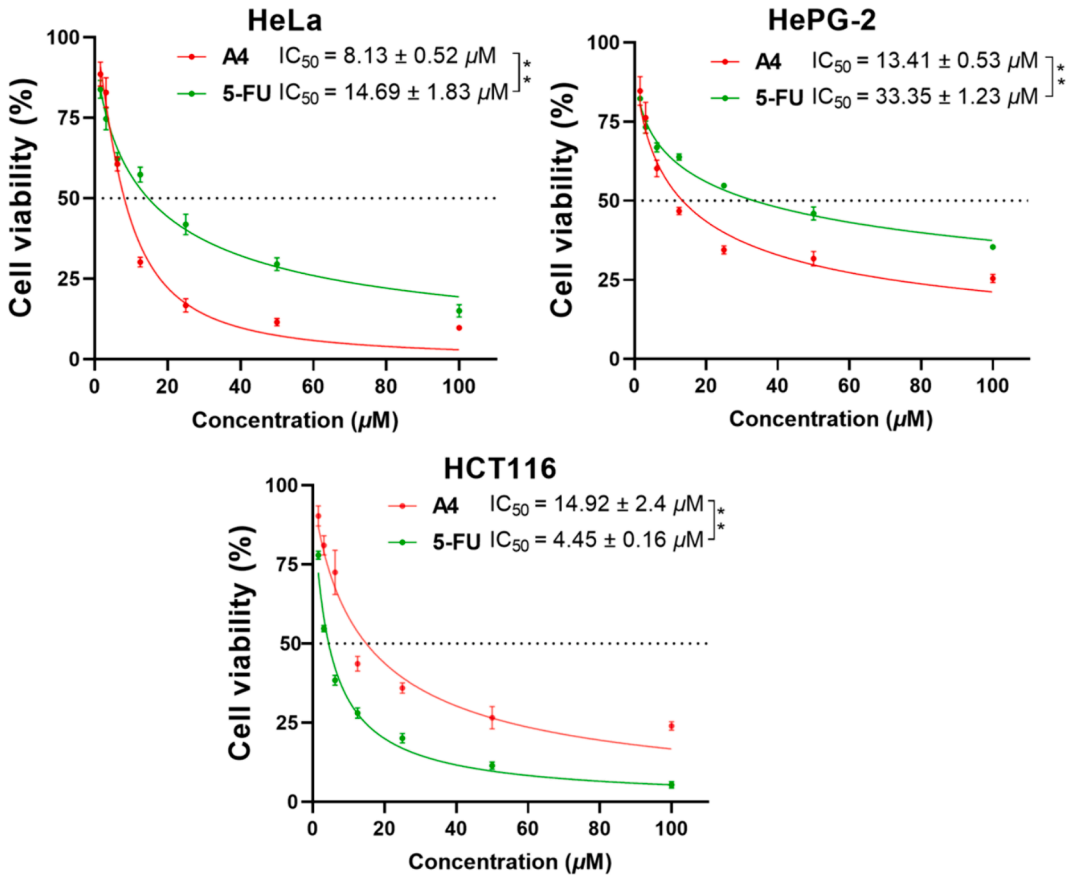

Fig. 5. IC_{50} values of compound **A4** and **5-FU** against three cancer cells. (** $p < 0.01$).

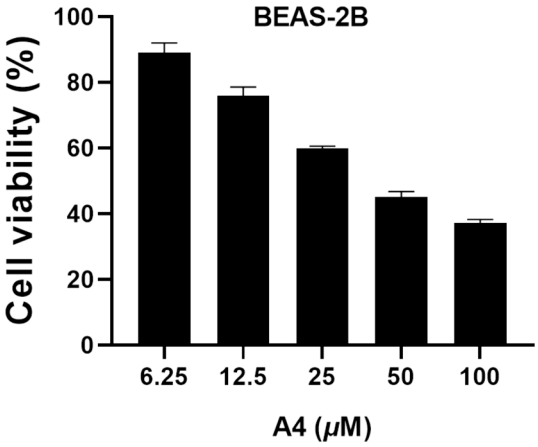

Fig. 6. Cell viability of BEAS-2B treated with compound **A4**.

2018). Among them, six compounds **A4**, **A7**, **B2**, **B5**, **B6** and **C5** inhibited AB with inhibition rates higher than 50 %. Compounds **A4**, **A7**, **B2**, and **C5** exhibited better effectiveness with inhibition rates exceeding 67 % against the AA strain, surpassing Kre (64.3 %). For CG strain, compounds **B2** (65.3 %), **C2** (65.3 %), **C3** (66.7 %), **C5** (86.1 %), **C6** (75.0 %) and **C8** (59.7 %) displayed higher antifungal activities than Kre (53 %). Furthermore, three compounds **A4** (58.3 %), **B13** (56.35) and **C5** (59.2 %) demonstrated slightly greater or comparable antifungal efficacy compared to Kre (53 %) for PG strain. Regrettably, nearly all of the desired substances showed weaker antifungal properties against the FV strain. In general, compound **C5** demonstrated a more favorable and wide-ranging antifungal impact compared to the agricultural fungicides **Kre**.

After analyzing the bioassay results mentioned earlier, certain structure–activity relationships (SARs) were examined as follow: (1) generally, introducing fluorine atom at C-6 and C-8 of coumarin was more beneficial for the improvement of the fungicigal activities (**A1** ~ **9**, **C1** ~ **11** *vs*. **B1** ~ **14**). (2) For compounds **A1** ~ **9**, the introduction of 1-ethylproyl group at **R** position led to a sharp increase in bioactivity, such as **A4**. (3) For compounds **B1** ~ **14**, adding n-propyl (**B2**) at the **R** position typically enhanced the antifungal effectiveness compared to other alkyl groups. (4) When the fluorine atom at the C-8 of coumarin, introduction of 1-ethylproyl group at **R** position could also obtain the best compound (**C5**). (5) Unfortunately, it was discovered that adding aromatic groups to the **R** position resulted in decreased potency for compounds **A8** ~ **9**, **B9** ~ **14** and **C9** ~ **11**. The findings of the aforementioned structure–activity relationship will serve as a theoretical guide for future optimization of the structure.

To further investigate the antifungal capabilities, the EC_{50} values of compound **C5** were examined against four phytopathogenic fungi (AB, AA, CG and PG) for more reliable results. As summarized in Table 2, this compound showed strong antifungal effects, with EC_{50} values ranging from 11.5 to 36.5 μg/mL. Particularly, compound **C5** exhibited superior fungicidal activity against AA, CG, and PG strains, with EC_{50} values of 11.5, 18.0, and 33.8 μg/mL, significantly lower than Kre (AA: 15.5 μg/mL, BC: 21.5 μg/mL, PG: 53.7 μg/mL).

3.3. *Molecular docking studies*

Chitinase, a key enzyme in chitin production, plays a vital part in breaking down external chitin, as well as in degrading and restructuring fungal cell walls (Hartl et al., 2012). Literature studies have shown that amidocoumarins exhibit notable chitinase inhibitory effects and possess

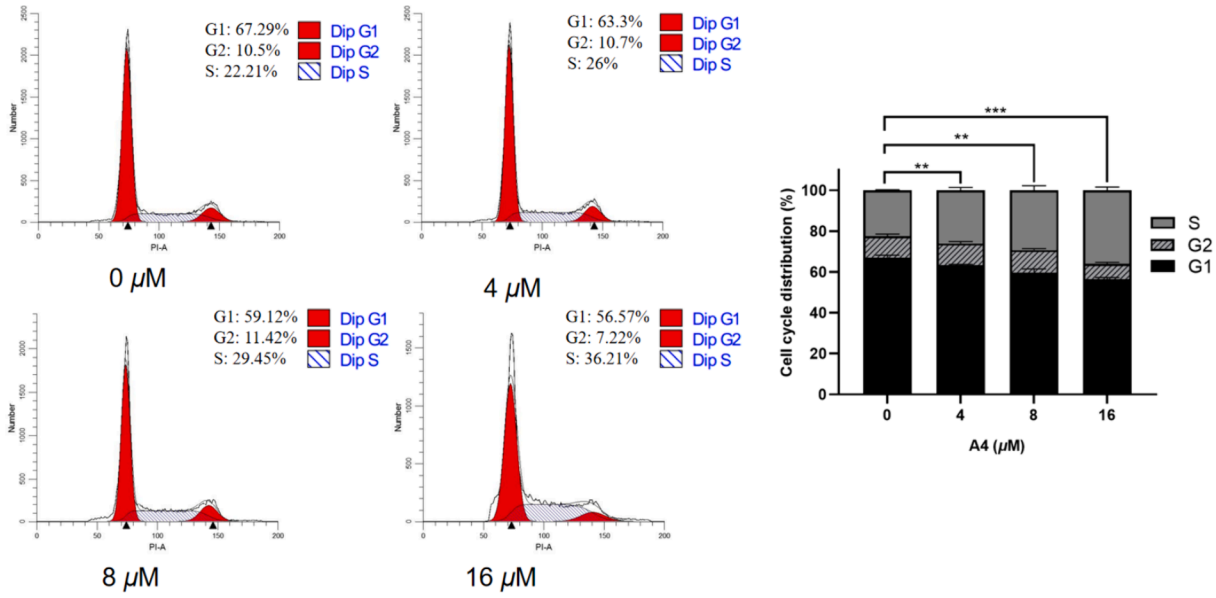

Fig. 7. Effect of compound **A4** on cell cycle in Hela cells. Flow cytometry of Hela cells treated with **A4** for 48 h. (** $p < 0.01$, *** $p < 0.001$).

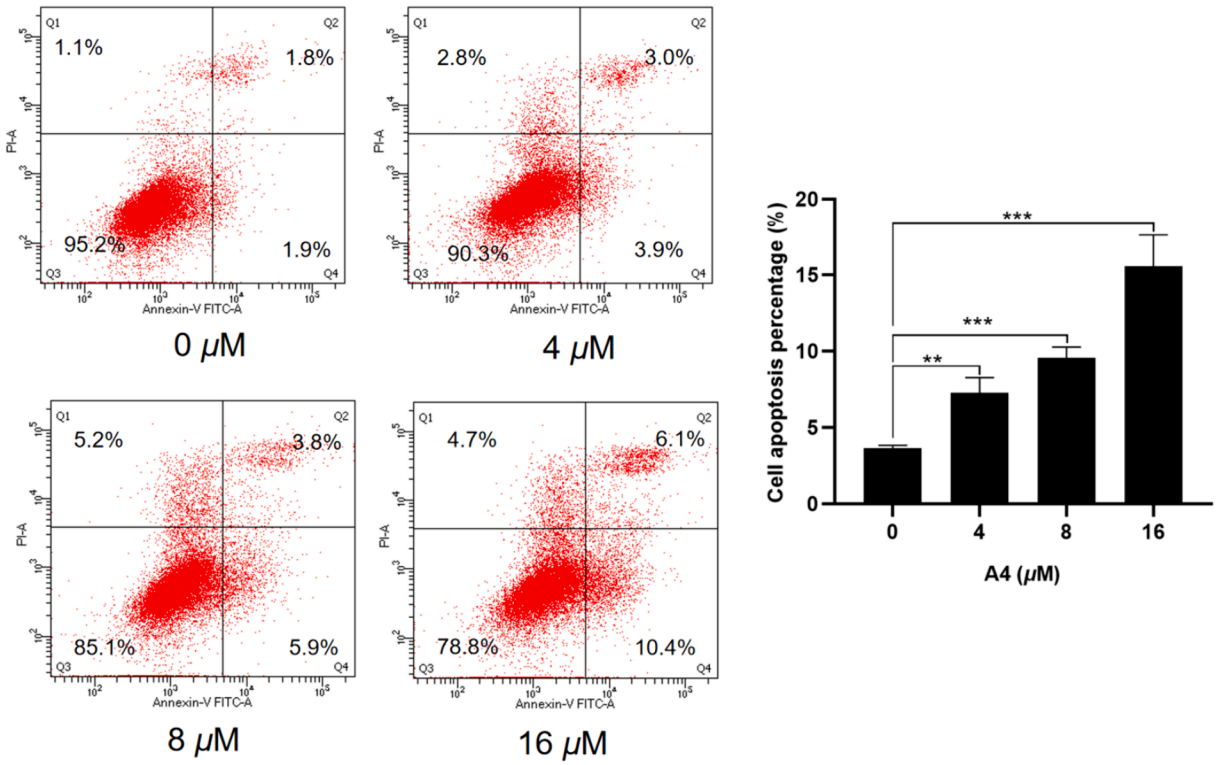

Fig. 8. Effect of compound **A4** on cell apoptosis in Hela cells. Flow cytometric analysis of apoptotic cells after treatment of Hela cells with **A4** for 48 h. (** $p < 0.01$, *** $p < 0.001$).

strong binding affinity to the receptor (Sharma et al., 2020). At present, molecular docking are commonly utilized in the study of natural products (López-López et al., 2021). Therefore, we employed molecular docking to investigate the binding interactions between compound **C5** and chitinase models in order to explore potential antifungal mechanisms.

Docking studies were conducted with AutoDock Tools (ADT) to explain the inhibitory activity of chitinase, utilizing a well-classified chitinase (PDB code: 1W9U) as the reference model. The docking result displayed that **C5** had good binding affinity to chitinase with the docking binding energies of −7.42 kcal/mol. As shown in Fig. 4, **C5** displayed hydrogen bonds and van der Waals attractions with polar residues within the binding cavity (Fig. 4, **A**), and shared similar binding modes with argadin, a natural chitinase inhibitor (Fig. 4, **B**) (Arai et al., 2000). The two carbonyl groups of **C5** formed hydrogen bonds with residues GLY221 and LYS224, respectively. The coumarin ring of **C5** had pi-sulfur interaction with MET243, pi-pi T-shaped interaction with TYR178, pi-alkyl interaction with PRO219. The fluorine atom formed halogen bond with MET243 and SER218 with bond length of 3.49 and 3.45 Å, respectively. The outcome suggested that the specific compound

C5 perfectly matched the active site and had a positive interaction with chitinase.

3.4. Anticancer activity

The synthesized compounds were evaluated for their anticancer properties at a concentration of 100 μmol/L on three human cancer cell lines: HeLa, HePG-2, and HCT116, and the results are collected in Table 3. Among these compounds, **A4** demonstrated the highest effectiveness in inhibiting the growth of the three cancer cells, with rates of 90.28 %, 73.58 %, and 76.01 %, respectively. Additionally, several other compounds showed satisfactory cytotoxic effects on other cancer cells. For example, **A2**, **A9**, **B2**, **B3** and **C11** caused Hela cells growth inhibition rates exceeding 50 %. Compounds **A2** and **A7** showed moderate effectiveness in inhibiting cell growth in HePG-2 cells, with inhibition rates of 53.02 % and 50.14 %, respectively. On the other hand, all the target compounds exhibited poorer anticancer activities against HCT116 cells except **A4**. SARs indicated that introducing fluorine atom at C-6 of coumarin was more beneficial for the improvement of the anticancer activities. When the fluorine atom at the C-6 of coumarin, introducing of pentan-3-yl group at **R** position had positive influence on the anticancer activities.

In addition, as shown in Fig. 5, the compound **A4** with the best anticancer activities were further examined to determine its IC_{50} against the three cancer cells, and the result delivered that it exhibited intriguing and remarkable profiles of inhibiting cell growth with IC_{50} values of 8.13 μM, 13.41 μM and 14.92 μM against Hela, HePG-2 and HCT116 cells, respectively, Approaching or exceeding the IC_{50} values of **5-FU** (14.69 μM, 33.35 μM and 4.45 μM). Moreover, **A4** was further evaluated for its cytotoxic activity against normal cells BEAS-2B. As depicted in Fig. 6**, A4** showed relative low cytotoxicity to BEAS-2B cells, and the IC_{50} values was over 45 μM. This result indicated that **A4** showed greater preference for cancer cells over human normal cells.

3.5. Cell cycle analysis

Building on the promising results from the initial in vitro antiproliferative tests, we delved deeper into the effects of **A4** on the cell cycle advancement of Hela cells through flow cytometry analysis. During the study, Hela cells were exposed to different amounts of **A4** (0, 4, 8, 16 μM) for 48 h. As shown in Fig. 7, In the presence of **A4**, the proportion of cancer cells in the S phase was 26 %, 29.45 %, and 36.21 %, compared to 22.21 % in the control group. The results showed that **A4** caused a significant S-phase arrest in a concentration-dependent manner.

3.6. Cell apoptosis analysis

Additionally, Hela cells were subjected to increasing doses of **A4** (0, 4, 8, 16 μM) for cell apoptosis assessment. As shown in Fig. 8, after incubating with **A4** for 48 h, the combined proportion of Q2 and Q4 apoptotic cells was 6.9 %, 9.7 %, and 16.5 %, respectively. On the other hand, the group that was not treated showed only 3.7 % of cells undergoing apoptosis. As a result, it was shown that compound **A4** had the ability to inhibit cell growth by causing cellular apoptosis.

4. Conclusion

In general, thirty-four novel coumarin amide derivatives bearing fluorine were prepared and their structures were elucidated through ^{1}H NMR, ^{13}C NMR and HRMS analyses. X-ray diffraction confirmed the structures of four compounds definitively. The antifungal assays showed that derivative **C5** exhibited outstanding antifungal activities. Molecular docking studies displayed **C5** had the good binding interactions with the target protein, chitinase. Moreover, three cancer cell lines were used to test the cytotoxic effects of the target compounds, and compound **A4** display the best cytotoxic activity against Hela cells with an IC_{50} value of 8.13 μM, while demonstrating low cytotoxicity against BEAS-2B. Additional mechanistic investigations demonstrated that **A4** could effectively halt the cell cycle during the S phase and trigger apoptosis. The findings indicate that these two new coumarin compounds may provide a promising option for fungicides and anticancer drugs.

CRediT authorship contribution statement

Xin Xiang: Writing – original draft, Methodology, Investigation, Formal analysis, Data curation. **Yafang Chen:** Writing – original draft, Methodology, Investigation, Formal analysis, Data curation, Conceptualization. **Lang Wu:** Investigation, Data curation, Conceptualization. **Long Zhang:** Investigation, Data curation. **Yan Zhang:** Methodology, Investigation, Formal analysis. **Wude Yang:** Writing – review & editing, Supervision, Project administration, Methodology. **Xiang Yu:** Writing – review & editing, Supervision, Project administration, Methodology, Formal analysis.

Declaration of competing interest

The authors declare that they have no known competing financial interests or personal relationships that could have appeared to influence the work reported in this paper.

Acknowledgements

This work was supported by the National Natural Science Foundation of China (82260833), Guizhou Provincial Natural Science Foundation [QKHJ-ZK(2022)YB503], Science and Technology Planning Project of Guizhou Province [QKHF-ZK(2023)G426]. The authors thank B.B. Chen for the chemical synthesis support.

Appendix A. Supplementary data

Supplementary data to this article can be found online at https://doi.org/10.1016/j.arabjc.2024.105872.

References

Akwu, N.A., Lekhooa, M., Deqiang, D., Aremu, A.O., 2023. Antidepressant effects of coumarins and their derivatives: a critical analysis of research advances. Eur. J. Pharmacol. 956, 175958 https://doi.org/10.1016/j.ejphar.2023.175958.

Alzahrani, S.M., Al Doghaither, H.A., Al-Ghafari, A.B., Pushparaj, P.N., 2023. 5–Fluorouracil and capecitabine therapies for the treatment of colorectal cancer (Review). Oncol. Rep. 50 (4), 175. https://doi.org/10.3892/or.2023.8612.

Arai, N., Shiomi, K., Yamaguchi, Y., Masuma, R., Iwai, Y., Turberg, A., Kölbl, H., Omura, S., 2000. Argadin, a new chitinase inhibitor, produced by Clonostachys sp. FO-7314. Chem. Pharm. Bull. (tokyo) 48 (10), 1442–1446. https://doi.org/10.1248/cpb.48.1442.

Awaad, A.S., Al-Jaber, N.A., Soliman, G.A., Al-Outhman, M.R., Zain, M.E., Moses, J.E., El-Meligy, R.M., 2012. New biological activities of *Casimiroa edulis* leaf extract and isolated compounds. Phytother Res. 26 (3), 452–457. https://doi.org/10.1002/ptr.3690.

Bizzarri, B.M., Botta, L., Capecchi, E., Celestino, I., Checconi, P., Palamara, A.T., Nencioni, L., Saladino, R., 2017. Regioselective IBX-mediated synthesis of coumarin derivatives with antioxidant and anti-influenza activities. J. Nat. Prod. 80 (12), 3247–3254. https://doi.org/10.1021/acs.jnatprod.7b00665.

Cavaliere, A., Probst, K.C., Westwell, A.D., Slusarczyk, M., 2017. Fluorinated nucleosides as an important class of anticancer and antiviral agents. Future Med. Chem. 9 (15), 1809–1833. https://doi.org/10.4155/fmc-2017-0095.

Deeks, E.D., 2018. Bictegravir/emtricitabine/tenofovir alafenamide: a review in HIV-1 infection. Drugs 78 (17), 1817–1828. https://doi.org/10.1007/s40265-018-1010-7.

Deshpande, S.R., Pai, K.V., 2012. Fluorine bearing sydnones with styryl ketone group: synthesis and their possible analgesic and anti-inflammatory activities. J. Enzyme Inhib. Med. Chem. 27 (2), 241–248. https://doi.org/10.3109/14756366.2011.586345.

Duan, Y.C., Ma, Y.C., Zhang, E., Shi, X.J., Wang, M.M., Ye, X.W., Liu, H.M., 2013. Design and synthesis of novel 1,2,3-triazole-dithiocarbamate hybrids as potential anticancer agents. Eur. J. Med. Chem. 62, 11–19. https://doi.org/10.1016/j.ejmech.2012.12.046.

Gao, L., Wang, F., Chen, Y., Li, F., Han, B., Liu, D., 2021. The antithrombotic activity of natural and synthetic coumarins. Fitoterapia 154, 104947. https://doi.org/10.1016/j.fitote.2021.104947.

Han, S., Lu, Y., 2023. Fluorine in anti-HIV drugs approved by FDA from 1981 to 2023. Eur. J. Med. Chem. 258, 115586 https://doi.org/10.1016/j.ejmech.2023.115586.
Hartl, L., Zach, S., Seidl-Seiboth, V., 2012. Fungal chitinases: diversity, mechanistic properties and biotechnological potential. Appl. Microbiol. Biotechnol. 93 (2), 533–543. https://doi.org/10.1007/s00253-011-3723-3.
Huang, G.Y., Cui, H., Lu, X.Y., Zhang, L.D., Ding, X.Y., Wu, J.J., Duan, L.X., Zhang, S.J., Liu, Z., Zhang, R.R., 2021. (+/-)-Dievodialetins A-G: seven pairs of enantiomeric coumarin dimers with anti-acetylcholinesterase activity from the roots of *Evodia lepta* Merr. Phytochemistry 182, 112597. https://doi.org/10.1016/j.phytochem.2020.112597.
Hunter, L., 2010. The C-F bond as a conformational tool in organic and biological chemistry. Beilstein J. Org. Chem. 6, 38. https://doi.org/10.3762/bjoc.6.38.
Ismail, F.M.D., 2002. Important fluorinated drugs in experimental and clinical use. J. Fluorine Chem. 118 (1–2), 27–33. https://doi.org/10.1016/S0022-1139(02)00201-4.
Jeschke, P., 2004. The unique role of fluorine in the design of active ingredients for modern crop protection. Chembiochem 5 (5), 571–589. https://doi.org/10.1002/cbic.200300833.
Jeschke, P., 2017. Latest generation of halogen-containing pesticides. Pest Manag. Sci. 73 (6), 1053–1066. https://doi.org/10.1002/ps.4540.
Kassim, N.K., Rahmani, M., Ismail, A., Sukari, M.A., Ee, G.C., Nasir, N.M., Awang, K., 2013. Antioxidant activity-guided separation of coumarins and lignan from *Melicope glabra* (Rutaceae). Food Chem. 139 (1–4), 87–92. https://doi.org/10.1016/j.foodchem.2013.01.108.
Küpeli Akkol, E., Genç, Y., Karpuz, B., Sobarzo-Sánchez, E., Capasso, R., 2020. Coumarins and coumarin-related compounds in pharmacotherapy of cancer. Cancers (basel). 12 (7), 1959. https://doi.org/10.3390/cancers12071959.
Li, Y., Luo, B., Luo, Z., Ma, T., Fan, L., Liu, W., Fan, J., Guo, B., Xue, W., Tang, L., 2023. Design and synthesis of novel 2,2-dimethylchromene derivatives as potential antifungal agents. Mol. Divers. 27 (2), 589–601. https://doi.org/10.1007/s11030-022-10421-9.
Liu, W., Li, Y., Fan, J., Tang, L., Guo, B., Xue, W., Fan, L., 2022. Natural products-based fungicides: synthesis and antifungal activity against plant pathogens of 2H-chromene derivatives. Chem. Biodivers. 19 (11), e202200802 https://doi.org/10.1002/cbdv.202200802.
Liu, Y.P., Yan, G., Xie, Y.T., Lin, T.C., Zhang, W., Li, J., Wu, Y.J., Zhou, J.Y., Fu, Y.H., 2020. Bioactive prenylated coumarins as potential anti-inflammatory and anti-HIV agents from *Clausena lenis*. Bioorg. Chem. 97, 103699 https://doi.org/10.1016/j.bioorg.2020.103699.
Longley, D.B., Harkin, D.P., Johnston, P.G., 2003. 5-Fluorouracil: mechanisms of action and clinical strategies. Nat. Rev. Cancer. 3 (5), 330–338. https://doi.org/10.1038/nrc1074.
López-López, E., Bajorath, J., Medina-Franco, J.L., 2021. Informatics for chemistry, biology, and biomedical sciences. J. Chem. Inf. Model. 61 (1), 26–35.
Luan, M.Z., Zhang, X.F., Yang, Y., Meng, Q.G., Hou, G.G., 2023. Anti-inflammatory activity of fluorine-substituted benzo[h]quinazoline-2-amine derivatives as NF-κB inhibitors. Bioorg. Chem. 132, 106360 https://doi.org/10.1016/j.bioorg.2023.106360.
Lv, H.N., Wang, S., Zeng, K.W., Li, J., Guo, X.Y., Ferreira, D., Zjawiony, J.K., Tu, P.F., Jiang, Y., 2015. Anti-inflammatory coumarin and benzocoumarin derivatives from *Murraya alata*. J. Nat. Prod. 78 (2), 279–285. https://doi.org/10.1021/np500861u.
Ma, H., Wang, K., Wang, B., Wang, Z., Liu, Y., Wang, Q., 2024. Design, synthesis, and biological activities of novel coumarin derivatives as pesticide candidates. J. Agric. Food Chem. 72 (9), 4658–4668. https://doi.org/10.1021/acs.jafc.3c08161.
Maleki, E.H., Bahrami, A.R., Sadeghian, H., Matin, M.M., 2020. Discovering the structure-activity relationships of different *O*-prenylated coumarin derivatives as effective anticancer agents in human cervical cancer cells. Toxicol. In Vitro. 63, 104745 https://doi.org/10.1016/j.tiv.2019.104745.
Paik, J., 2021. Teriflunomide: pediatric first approval. Paediatr. Drugs. 23 (6), 609–613. https://doi.org/10.1007/s40272-021-00471-1.
Phutdhawong, W., Chuenchid, A., Taechowisan, T., Sirirak, J., Phutdhawong, W.S., 2021. Synthesis and biological activity evaluation of coumarin-3-carboxamide derivatives. Molecules 26 (6), 1653. https://doi.org/10.3390/molecules26061653.
Poulakos, M., Grace, Y., Machin, J.D., Dorval, E., 2017. Efinaconazole and tavaborole. J. Pharm. Pract. 30 (2), 245–255. https://doi.org/10.1177/0897190016630904.
Prusty, J.S., Kumar, A., 2020. Coumarins: antifungal effectiveness and future therapeutic scope. Mol. Divers. 24 (4), 1367–1383. https://doi.org/10.1007/s11030-019-09992-x.
Purser, S., Moore, P.R., Swallow, S., Gouverneur, V., 2008. Fluorine in medicinal chemistry. Chem. Soc. Rev. 37 (2), 320–330. https://doi.org/10.1039/B610213C.
Sakunpak, A., Matsunami, K., Otsuka, H., Panichayupakaranant, P., 2013. Isolation of new monoterpene coumarins from Micromelum minutum leaves and their cytotoxic activity against Leishmania major and cancer cells. Food Chem. 139 (1–4), 458–463. https://doi.org/10.1016/j.foodchem.2013.01.031.
Santos Junior, C.M., Silva, S.M.C., Sales, E.M., Velozo, E.D.S., Dos Santos, E.K.P., Canuto, G.A.B., Azeredo, F.J., Barros, T.F., Biegelmeyer, R., 2023. Coumarins from Rutaceae: chemical diversity and biological activities. Fitoterapia 168, 105489. https://doi.org/10.1016/j.fitote.2023.105489.
Sharma, R.K., Singh, V., Tiwari, N., Butcher, R.J., Katiyar, D., 2020. Synthesis, antimicrobial and chitinase inhibitory activities of 3-amidocoumarins. Bioorg. Chem. 98, 103700 https://doi.org/10.1016/j.bioorg.2020.103700.
Siskos, E.P., Mazomenos, B.E., Konstantopoulou, M.A., 2008. Isolation and identification of insecticidal components from *Citrus aurantium* fruit peel extract. J. Agric. Food Chem. 56 (14), 5577–5581. https://doi.org/10.1021/jf800446t.
Song, P.P., Zhao, J., Liu, Z.L., Duan, Y.B., Hou, Y.P., Zhao, C.Q., Wu, M., Wei, M., Wang, N.H., Lv, Y., Han, Z.J., 2017. Evaluation of antifungal activities and structure-activity relationships of coumarin derivatives. Pest Manag. Sci. 3 (1), 94–101. https://doi.org/10.1002/ps.4422.
Tan, N., Yazıcı-Tütüniş, S., Bilgin, M., Tan, E., Miski, M., 2017. Antibacterial activities of pyrenylated coumarins from the roots of *Prangos hulusii*. Molecules 22 (7), 1098. https://doi.org/10.3390/molecules22071098.
Tang, Z.H., Liu, Y.B., Ma, S.G., Li, L., Li, Y., Jiang, J.D., Qu, J., Yu, S.S., 2016. Antiviral spirotriscoumarins A and B: two pairs of oligomeric coumarin enantiomers with a spirodienone-sesquiterpene skeleton from *Toddalia asiatica*. Org. Lett. 18 (19), 5146–5149. https://doi.org/10.1021/acs.orglett.6b02572.
Tuan Anh, H.L., Kim, D.C., Ko, W., Ha, T.M., Nhiem, N.X., Yen, P.H., Tai, B.H., Truong, L.H., Long, V.N., Gioi, T., Hong Quang, T., Minh, C.V., Oh, H., Kim, Y.C., Kiem, P.V., 2017. Anti-inflammatory coumarins from *Paramignya trimera*. Pharm. Biol. 55 (1), 1195–1201. https://doi.org/10.1080/13880209.2017.1296001.
Yang, R., Liu, Z., Han, M., Cui, L., Guo, Y., 2022. Preparation and biological evaluation of novel osthole-derived *n*-benzoylthioureas as insecticide candidates. J. Agric. Food Chem. 70 (50), 15737–15746. https://doi.org/10.1021/acs.jafc.2c06558.
Yang, R., Cheng, W., Huang, M., Xu, T., Zhang, M., Liu, J., Qin, S., Guo, Y., 2024. Novel membrane-targeting isoxanthohumol-amine conjugates for combating methicillin-resistant Staphylococcus aureus (MRSA) infections. Eur. J. Med. Chem. 268, 116274 https://doi.org/10.1016/j.ejmech.2024.116274.
Yu, X., Teng, P., Zhang, Y.L., Xu, Z.J., Zhang, M.Z., Zhang, W.H., 2018. Design, synthesis and antifungal activity evaluation of coumarin-3-carboxamide derivatives. Fitoterapia 127, 387–395. https://doi.org/10.1016/j.fitote.2018.03.013.
Yu, X., Zhao, Y.F., Huang, G.J., Chen, Y.F., 2021. Design and synthesis of 7-diethylaminocoumarin-based 1,3,4-oxadiazole derivatives with anti-acetylcholinesterase activities. J. Asian Nat. Prod. Res. 23 (9), 866–876. https://doi.org/10.1080/10286020.2020.1803293.
Zhang, Z., Bai, Z.W., Ling, Y., He, L.Q., Huang, P., Gu, H.P., Hu, R.F., 2018. Design, synthesis and biological evaluation of novel furoxan-based coumarin derivatives as antitumor agents. Med. Chem. Res. 27, 1198–1205. https://doi.org/10.1007/s00044-018-2140-x.
Zhao, L.X., Chen, K.Y., Zhao, H.Y., Zou, Y.L., Gao, S., Fu, Y., Ye, F., 2023. Design, synthesis and biological activity determination of novel phenylpyrazole protoporphyrinogen oxidase inhibitor herbicides. Pestic. Biochem. Physiol. 196, 105588 https://doi.org/10.1016/j.pestbp.2023.105588.
Zuo, G.Y., Wang, C.J., Han, J., Li, Y.Q., Wang, G.C., 2016. Synergism of coumarins from the Chinese drug Zanthoxylum nitidum with antibacterial agents against methicillin-resistant *Staphylococcus aureus* (MRSA). Phytomedicine 23 (14), 1814–1820. https://doi.org/10.1016/j.phymed.2016.11.001.